𝕬𝖗𝖌𝖔𝖓𝖓𝖊 𝕹𝖆𝖙𝖎𝖔𝖓𝖆𝖑 𝕷𝖆𝖇𝖔𝖗𝖆𝖙𝖔𝖗𝖞

REACTOR DEVELOPMENT PROGRAM

PROGRESS REPORT

May 1963

ARGONNE NATIONAL LABORATORY
9700 South Cass Avenue
Argonne, Illinois

REACTOR DEVELOPMENT PROGRAM
PROGRESS REPORT

May 1963

Albert V. Crewe, Laboratory Director

Division	Director
Chemical Engineering	S . Lawroski
Idaho	M. Novick
Metallurgy	F . G. Foote
Reactor Engineering	B . I . Spinrad
Remote Control	R . C. Goertz

Report coordinated by
R. M. Adams and A. Glassner

Issued June 15, 1963

FOREWORD

The Reactor Development Program Progress Report, issued monthly, is intended to be a means of reporting those items of significant technical progress which have occurred in both the specific reactor projects and the general engineering research and development programs. The report is organized in a way which, it is hoped, gives the clearest, most logical over-all view of progress. The budget classification is followed only in broad outline, and no attempt is made to report separately on each sub-activity number. Further, since the intent is to report only items of significant progress, not all activities are reported each month. In order to issue this report as soon as possible after the end of the month editorial work must necessarily be limited. Also, since this is an informal progress report, the results and data presented should be understood to be preliminary and subject to change unless otherwise stated.

The issuance of these reports is not intended to constitute publication in any sense of the word. Final results either will be submitted for publication in regular professional journals or will be published in the form of ANL topical reports.

TABLE OF CONTENTS

TABLE OF CONTENTS

iv

TABLE OF CONTENTS

I. BOILING WATER REACTORS

A. BORAX-V

1. Reactor Operations

Room-temperature, zero-power experiments with the core having the central superheater have been performed. These include a preliminary measurement of the reactivity effect of temperature, the rate of water leakage from the boiling region to the superheater region for open-vessel operating conditions, and the reactivity effect of flooding the superheater, as well as flux-wire irradiations for determining neutron-flux distributions without boric acid in the moderator water.

The reactor temperature was raised from 78 to 123°F by means of the electric preheat system. The temperature was then lowered to 107°F by diluting reactor water with cool water. Comparison of the change in the critical positions of the control bank at temperatures of 78°F and 107°F indicated a small, negative reactivity effect of about 0.001% per °F.

The leakage rate of water from the boiler to the superheater region was determined. Beams were installed across the reactor vessel flange in place of the reactor vessel head to compress the hold-down springs for the superheater fuel assemblies, thereby providing the design force on the O-ring seals on the bottom of the fuel assemblies. Initial tests revealed an excessive leak rate. Most of this leakage was found to be caused by unsatisfactory welds at the joining of the fuel elements to the riser and the nozzle of six assemblies. After these welds were repaired and leak-tested with 1 to 3 lb of air pressure on the steam side of the assembly, a leakage rate of about 1 gal/hr was obtained for the core loaded with three temporary superheater fuel assemblies having taped, detachable nozzles and nine standard, finished-welded assemblies. This rate will be acceptable for superheat operation.

The reactivity effect of flooding the superheater was determined by finding the change in control rod position with water level in the superheater at several different heights. The measurements indicated that the reactivity effect of draining the superheater steam channels is about -0.9% with all control rods banked near 10.5 in., and about -1.2% with the central control rod fully withdrawn and the remaining eight control rods banked near 9.5 in.

Five reactor runs were made for the irradiation of flux wires to determine the effects on flux distribution of changes in position of the central control rod with the superheater both flooded and drained.

2. Analysis

a. <u>Power Distribution</u>. Gamma-scanning of 15 boiling fuel rods irradiated at 15 Mw in boiling core B-2 was completed. There was good internal consistency among the results for the 15 fuel rods. There also appeared to be satisfactory agreement between these results and the fine neutron flux distribution measurements made in the cold boiling core after reasonable corrections had been made to the cold measurements.

The measured local peak-to-average power in core B-2 at 15 Mw was 1.96, and extrapolation to the fuel rod which is believed to be the hottest, yielded an estimated maximum peak-to-average power of about 2.43 as compared with the value of 2.77 reported for core B-1B.[1]

b. <u>Transfer Function</u>. A theoretical, distributed-parameter model has been derived for calculating dynamic temperatures in the BORAX-V superheater. In particular, both steam and fuel temperatures (vs. axial position) can be determined in each pass as a function of super-heater power and steam flow for the following cases:

(i) oscillating the reactor by rod oscillator at power, and

(ii) step changes in reactor power or steam flow.

Thus, in (i) above, the amplitudes of superheater temperatures can be determined as a function of the input reactivity amplitude at the various oscillator frequencies. In (ii) above, the time response of superheater temperatures to step changes in reactor power or steam flow can be evaluated. The constants in the model can be readily changed to calculate all of the above at various values of mean reactor power and mean reactor steam flow.

The transfer functions relating steam and fuel temperatures to reactor power and steam flow have been coded for the IBM-1620 to calculate (i) above. An additional IBM-1620 code has been written for the evaluation of the LaPlace Inversion Integral, which is used to calculate (ii) from the derived transfer functions.

3. Modification and Maintenance

The neutron-source drive was installed with the linear flux ion chamber positioned in a thimble in the reactor vessel to permit zero-power experiments at lower flux levels, thereby reducing the activation of the superheater fuel and improving the accuracy of critical and period measurements.

---

[1]R. E. Rice <u>et al</u>., Zero Power Experiments on Boiling Core B-1, BORAX-V, ANL-6689 (to be published).

A count-rate meter and recorder have been installed to record the neutron flux level during reactor shutdown.

The demineralizer resin for the reactor water was replaced to obtain higher efficiency in removal of residual boric acid. Procedures for accomplishing this were found to be satisfactory in all respects. Although the radioactivity level of this resin was only 50 mr/hr on contact, it appears evident that these procedures will be satisfactory for much higher radioactivity levels. The demineralizer was recharged with 8 ft^3 of ILCO-NR-6 resin.

Recirculation of reactor water through this fresh resin bed brought the reactor water quality up to a specific resistance of 2 megohm-cm. Also, the boric acid concentration was reduced from as high as 8 ppm to 0.094 ppm.

A flow-rate control orifice has been installed in the superheater-flood line to limit the rate of reactivity addition in the event of maloperation of the flooding system and failure of interlocks. At atmospheric pressure and room temperature, the time to raise the water level through the 2-ft height of the active core was approximately 62 sec.

The superheater flooding, draining, and water-level-measuring systems have been checked out and found to be satisfactory for operation at atmospheric conditions.

The packing gland on the auxiliary water pump has been replaced with a carbon-ring mechanical seal so as to reduce the maintenance that has been in the past required for this unit.

Three cartridge heaters and four strip heaters in the electric preheat system were burned out and have been replaced. Further revisions have been made in the electrical terminations for these heaters in an effort to keep them operative.

A differential pressure regulator is being installed in the water chemistry sample station to insure that the calomel electrode of the Beckman pH cell will not be accidentally back-pressured as it has been in the past. The thallium-column oxygen analyzer has been repaired. Preliminary checks with standardized conductivity solutions indicate that performance will probably be satisfactory.

4. Design, Fabrication, and Procurement

   a. Experimental Equipment. Electrical redesign of the modified H_2-O_2 recombiner, which now includes a new water decomposer and an associated circulating pump, was completed. Most materials for the modification are on hand, and rebuilding and wiring are in progress.

Construction of a 6-in.-dia x 18-ft-long, 600-psig, 489°F auto-clave for saturated water testing of in-vessel instruments and other com-ponents is nearing completion. Control and heater circuits have been checked out, the vessel has been hydrotested, and insulation has been installed.

Detailed design of a fueled, rotating oscillator rod has been completed and fabrication has started.

Detailed design of a plastic mockup of a spherical pellet, island moderator, superheater fuel assembly concept was completed. This mockup will be used as a test section for air-flow pressure-drop measurements.

b. Stainless Steel-clad Superheat Fuel. As mentioned in the April Progress Report (ANL-6717, p. 3), the Type 406 stainless steel-clad, enriched fuel plates being manufactured by Atomics International (AI) will be assembled at ANL.

Sufficient dummy fuel plates, side strips, and spacer wires have been nickel plated for two subassemblies. Both subassemblies will be vacuum brazed. Coast Metals 60 brazing alloy (1150°C flow point) will be used on one subassembly and Permabraze 128 brazing alloy (1000°C flow point) on the other. The evaluation of these two dummy subassemblies will be used as a basis for further development work as required.

In an attempt to fabricate a dummy pea-in-a-pod type fuel rod (see December Progress Report, ANL-6672, p. 6) some lengths of Type 406 stainless steel were filled with chrome alloy steel balls, end caps were welded to the tube ends, and the tubing was cold formed by isostatic press-ing around the balls. The balls remained tangent as desired. Longitudinal wrinkles were formed in the tubing between balls, however. It is quite likely that wrinkles such as these are potential sources of cladding cracks and ultimate failure in service.

5. Development and Testing

A scheme for in-core measurement of superheater water level has been successfully tried on a dummy fuel assembly. A technique was worked out to detect the level at five equally spaced points between the top and bottom of the superheater fuel by water-resistivity probes. Cir-cuits are being arranged to record the change in level in three fuel assemblies simultaneously during superheater flooding-time experiments.

Autoclave testing of a boiling fuel assembly box at 600 psig, and 489°F was terminated after 132 days. Inspection of the assembly indicated no evidence of failure of the "A" nickel rivets or of the X-8001 aluminum box, and there was no excessive corrosion.

The Type 304 stainless steel-clad UO_2 balls which were coated with Coast Metals 60 brazing alloy (see April Progress Report, ANL-6717, p. 4) have been corrosion tested for 17.5 days in oxygenated steam at 650°C, and 600 psi. Weight gains for the samples tested were 0.2 mg/cm^2 after 2.8 days and 1.0 mg/cm^2 after 17.5 days. By comparison, the weight gain of a Type 406 stainless steel plate specimen was about 0.3 mg/cm^2 after 13 days and 0.4 mg/cm^2 after 27 days under similar test conditions. Metallographic examination of some of the coated balls has shown that the thickness of the coating and the extent of diffusion of the brazing alloy into the Type 304 stainless steel are not uniform.

Available corrosion data on Type 304 stainless steel provide evidence that it corrodes at a faster rate than when coated with Coast Metals 60. The factor by which the two rates differ is not known, since corrosion of Type 304 stainless steel under superheated steam conditions appears to be dependent on the surface condition of the sample tested.

II. LIQUID-METAL-COOLED REACTORS

A. General Research and Development

1. ZPR-III

Experiments were continued this month with Assembly 43, the second two-zone reactor constructed in the ZPR-III. The assembly (see Progress Report for April 1963, ANL-6717, p. 6) consists of a dilute central region representing the center of a 4,000-liter, sodium-cooled power reactor, a radial buffer region, and an annular driver. The central core, filter, and driver are all 34.06 in. long, but the respective concentric effective radii are 9.61, 12.4, and 17.8 in. The central region has a low-density axial blanket with a composition similar to that of the core. The remainder of the assembly has a high-density blanket consisting of depleted uranium. The reactor became critical with 588.1 kg U^{235}. Of this, 72.06 kg was in the central core, 1.88 kg in the filter, and 514.16 kg in the driver. A cross section of the reactor is shown in Figure 1.
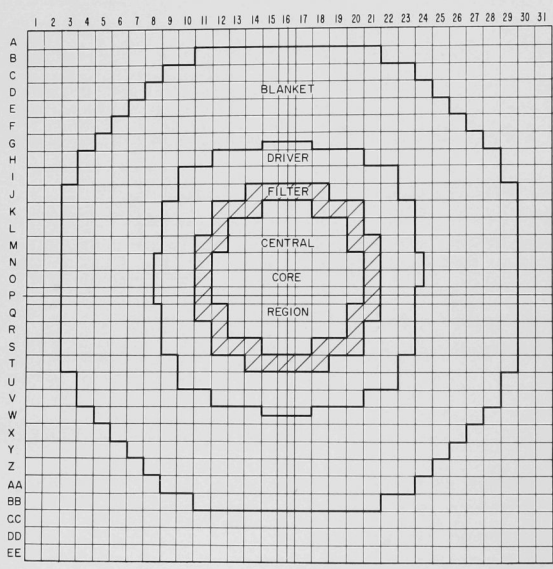
Figure 1

Outline of Core
of Assembly 43

a. Doppler Measurements. Equipment for Doppler measurements was completely installed and the final tests were being made when it was discovered that the uranium oxide fuel element was not heating properly. X radiographs showed that the element had expanded and broken the end fittings. New elements are being made at Argonne, Illinois

b.   Spectral Measurements. Seven different types of nuclear track plates, one of which was covered with cadmium, were irradiated. These have been sent to Northwestern University for analysis.

Additional fission ratio measurements were made, including those for U^{234}/U^{235}, Pu^{239}/Pu^{240}, and Pu^{240}/U^{235}. Some preliminary comparisons were made between thin-walled gas-flow, thick-walled gas-flow, and Kirn-type fission counters. Additional measurements will be performed with the gas-flow counters when a filter assembly is completed to filter the outlet gas from the counters.

Aluminum capsules containing sodium nitrate, natural and enriched uranium foils, and aluminum strips were irradiated for activation, fission, and capture measurements. The aluminum activates to Na^{24} by an (n, α) reaction with a threshold of about 6 Mev. The aluminum was irradiated to evaluate its worth as a threshold detector.

c.   Sodium-Void Coefficients. Measurements were performed to determine the worth of sodium at the center only, and for the full length of the core and axial blanket, for the configurations shown in Figure 2. The results (see Table I) indicated a negative worth, as expected, for the central value, but positive values were obtained for the full-length measurements.

(a) Sample regions for 2 central drawers (1 per half) and 18 central drawers (9 per half).

(b) Sample region for 10 central drawers (5 per half).
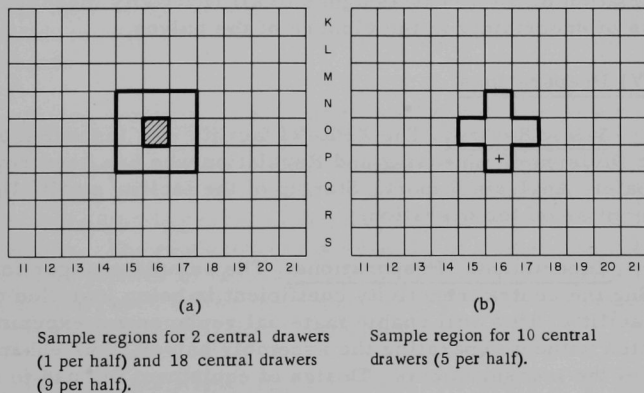
Figure 2. Arrangements for Measurement of Sodium-Void Coefficients

d.   Axial Worth Measurements. Presently, reactivity worths are being measured for core-length columns of various materials (niobium, tantalum, molybdenum, zirconium and all of the core materials) in the central region.

Table I. Sodium-Void Coefficients for Assembly 43 of ZPR-III

	Sodium Mass Removed (kg)	Reactivity Change (Ih ± 0.5)[a]	Worth of Sodium (Ih/kg)
A. Central Measurements			
2 Central Drawers	0.244	+ 0.3	-1.3 ± 2.0
10 Central Drawers	1.22	+ 1.6	-1.3 ± 0.4
18 Central Drawers	2.20	+ 1.33	-1.5 ± 0.3
B. Axial Measurements			
60% of Sodium Removed			
2 Central Drawers	1.203	- 1.1	+0.9 ± 0.4
10 Central Drawers	6.014	- 6.46	+1.09 ± 0.08
18 Central Drawers	10.825	+ 3.3	+1.06 ± 0.05
All Sodium Removed			
2 Central Drawers	2.005	- 2.15	+1.1 ± 0.3
10 Central Drawers	10.02	-10.6	+1.06 ± 0.05

[a] A variation of ± 0.5 Ih is assigned to all reactivity measurements because of uncertainty in the closure of the halves.

2. ZPR-VI Preparations

a. _Safety Review._ The ZPR-VI facility was inspected by a member of the Division of Licensing and Regulation who has been reviewing the ZPR-VI Safety Analysis Report. Startup of the facility awaits the approval by the Commission for operation.

b. _Experimental Preparations._ The sample changer for use in determining the central reactivity coefficient is being installed on the ZPR-VI facility. This will enable material replacement experiments to be conducted without separating the assembly halves, thus enhancing the accuracy of the measurements. Design of equipment for use in making a "fatman effect" measurement is in progress. Installation of necessary coaxial cables and wiring has been completed for the measurements of the prompt neutron period (Rossi alpha).

3. ZPR-IX Preparations

The ZPR-IX facility is scheduled for use in a series of critical experiments in connection with the nuclear rocket reactor program. The following work is being done to prepare the facility for operation.

a.   Cell Containment. In an effort to reduce leakage from the cell, a new seal channel is being designed for the inner door of the airlock. Unlike the other channel, which was fabricated from thin sheet steel, this will be milled from a solid piece. The much thicker walls will eliminate deflection under sealing pressures. In addition, the design is such as to locate the seal away from the edge of the door jamb and thus provide a better bearing surface.

b.   Facility Preparation. On the basis of tests, it was concluded that hard anodizing of the drawers would be sufficient, and that the tubes would not require this treatment. However, the bottom edges at the end of each tube will be rounded off to eliminate the scraping which results from contact with the sharp corners on the drawers. This will be done when the bundles are being stacked.

Assembly of the dual-purpose rod drives is proceeding, and testing has begun. A few units are just about ready for delivery. The beams for the support plate are almost ready for the paint shop.

c.   Procurement of Materials. Steel will be used as the non-moderating reflector material because it is inexpensive and readily available. Ordinary low-carbon steel consists almost completely of pure iron, with impurity concentrations being present as small fractions of a percent. The theoretical treatment required for the use of this material should be straightforward.

d.   Safety Analysis. The safety aspects of the proposed experiments appear to be straightforward, with the exception of those involving the axial moderating reflector. In the design, some of the horizontal matrix tubes in the core of the assembly are loaded with drawers containing fuel only and adjoining tubes are loaded with drawers containing both fuel and tungsten. The moderating material is, of course, placed in the ends of the outer drawer of the assembly to form the external reflector. Originally, it was expected that the expansion in the all-fuel rows would reduce the overall reactivity in the assembly.

The safety analysis now indicates that there is a net positive reactivity effect during transients, since, because the heating will primarily be in the fuel, the expansion in the all-fuel drawers will be greater than in the mixed drawer. Thus, the position of fuel in the all-fuel matrix tubes will change with respect to the reflector in a matrix tube containing fuel and tungsten. This change in relative position can result in an increase in reactivity. A possible solution to this problem may be found by alternating the all-fuel and mixed drawers in each matrix tube. This change will insure that more tungsten, which is an absorber, will be pushed towards the reflector along with the fuel, thus giving a negative overall effect.

Another problem with the axial moderating reflector is the uncertainty as to whether the reactivity effect of control-drawer withdrawal will be always negative. This problem will be studied further.

The data from the various aluminum matrix deflection tests have been studied. The behavior of tubes under load appears to be anomalous and does not fit simple models. Further study is required.

B. EBR-I

1. Experiments with Mark IV

The power level of EBR-I Mark IV has been raised in steps to a maximum of 1200 kw with low inlet temperature. Figure 3 shows the preliminary results of reactor transfer function measurements for zero power and full power. The amplitude, G, is indicated in arbitrary linear units. Analysis of the data has not been completed. However, these curves suffice to show that the reactor is stable, and particularly so at very low frequency. A small resonance is evident in the vicinity of 0.2 cps. No attempt has been made to date to separate and evaluate the various feedback effects.
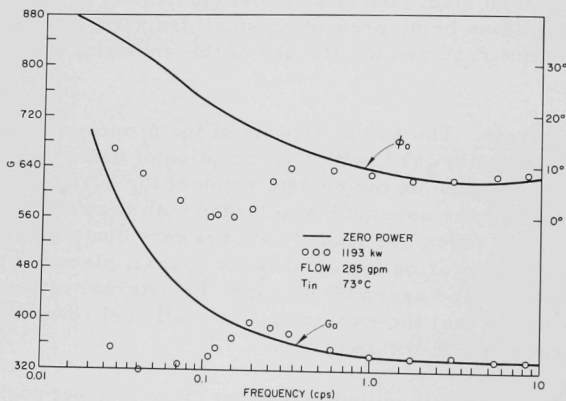
Figure 3

Transfer Function.
EBR-I, Mark IV.

In the course of experimentation, it has been observed that the total available reactivity referred to a standard set of conditions fluctuates from startup to startup. These fluctuations describe a pattern dependent on the modes of operation. Graphs in Figures 4 through 9 are given to indicate this pattern. Reactivity changes are reversible and contained within a total band width of approximately 100 Ih. Operation with low inlet temperature following previous high-temperature operation results in loss of available reactivity. Conversely, operation at the designed high temperature of the coolant results in a regain of this reactivity. Changes are

apparently independent of operating time for a particular run. There is some evidence that the reactivity gained from high-temperature operation comes into existence during the process of the reactor cooling off or, in other words, during the shutting-down process.
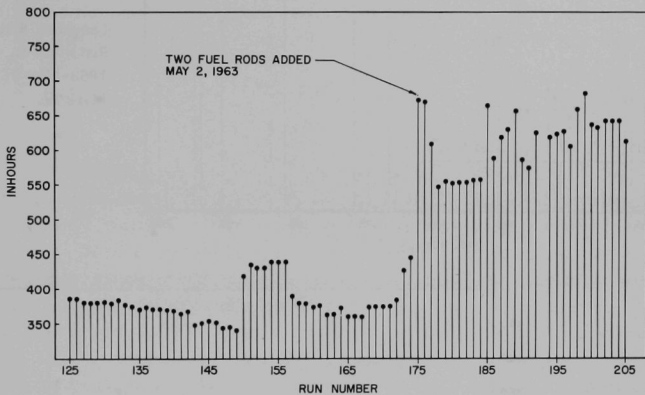
Figure 4. Inhours Available at 100°C, Critical vs. Startup Number. March 28, 1963-May 21, 1963. EBR-I, Mark IV.
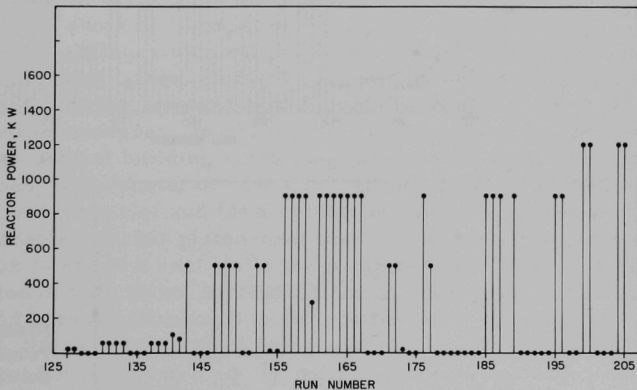
Figure 5. Reactor Power vs. Run Number. March 28, 1963-May 21, 1963. EBR-I, Mark IV.
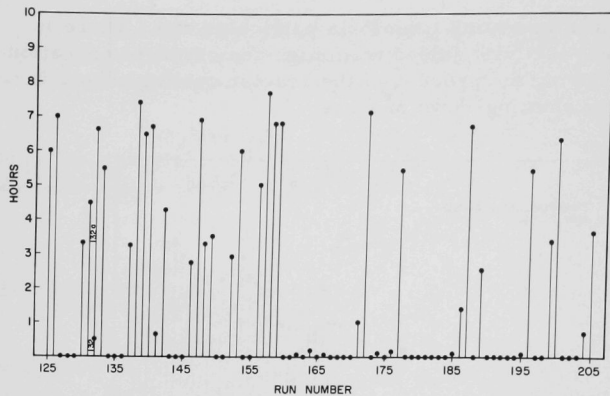
Figure 6

Length of Run in Hours vs. Run Number. March 28, 1963-May 21, 1963. EBR-I, Mark IV.

Figure 7

Maximum Fuel Rod Temperature vs. Run Number. March 28, 1963-May 21, 1963. EBR-I, Mark IV.
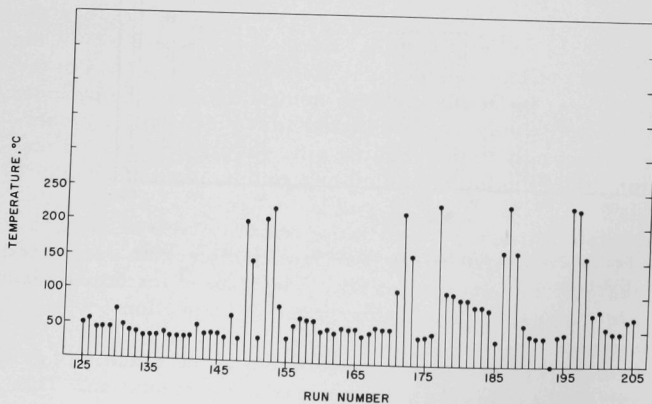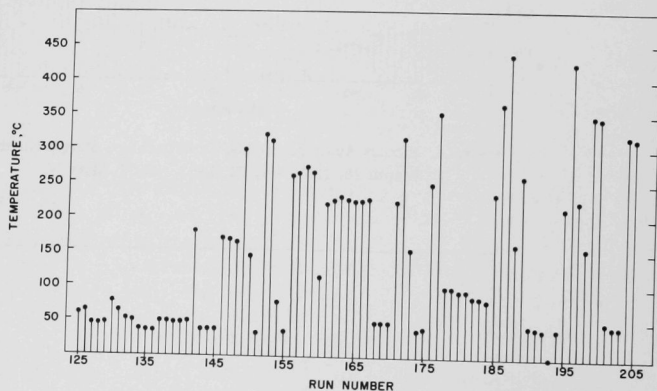
Figure 8

Maximum Inlet NaK Temperature vs. Run Number. March 28, 1963-May 21, 1963. EBR-I, Mark IV.
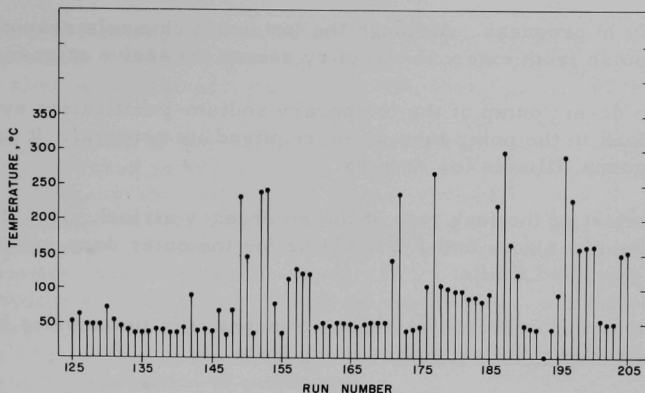
Figure 9. Maximum NaK Outlet Temperature vs. Run Number. March 28, 1963-
May 21, 1963. EBR-I, Mark IV.

C. EBR-II

1. Reactor Plant

Further investigation of the trouble with primary sodium pump
No. 1 (as noted in the Progress Report for April 1963, ANL-6717, p. 12)
failed to pinpoint the trouble sufficiently to warrant an attempt at any cor-
rective action short of removal of the pump. Equipment necessary for
removal of the pump, which will be a complex operation because of the
necessity for maintaining an inert gas atmosphere above the sodium in the
primary tank during removal of the pump, is being designed and fabricated.
It will also be necessary to protect the sodium-coated components of the
pump from normal building air during these operations. The major pieces
of equipment will consist of: (1) a transition piece connected between the
elliptical pump nozzle; and (2) a cylindrical shell, approximately 30 ft high,
with a movable internal piston-seal member which will be attached to the
crane hook to effect a seal while the pump is being lifted into the cylinder.
Fabrication of both items (except for the piston assembly) has been com-
pleted, and both are in transit to the reactor site. In preparation for the
operation, the primary tank is being cooled to a temperature of 250-300°F.

During the month, a vacuum distillation apparatus, to be used to
remove sodium from the circulating filter subassemblies, was assembled
and operationally tested. The equipment will also be used for future clean-
ing of nonradioactive subassemblies for purposes of inspection.

The first wet critical source was assembled in the reactor in grid
position 14-B-5 to permit checkout of the nuclear instrumentation. This

is currently in progress. Although the low-level channels respond satis-factorily, noise from external circuitry seems excessive at present.

The dc-em pump of the temporary sodium-purification system de-veloped a leak in the pump tube which required its removal. It has been sent to Argonne, Illinois for repairs.

A retest of the leak rate of the emergency airlock yielded 2.4 ft^3/24 hr for the inner door and 2.9 ft^3/24 hr for the outer door, which is well within the specified limits.

A system to provide an argon atmosphere in the annulus between the double-walled primary tank is being installed.

2. Sodium Boiler Plant

The vacuum distillation sodium-cleanup system was reassembled and tested at the EBR-II facility. The results show that all sodium was re-moved from the test sample and that the cleanup apparatus is operational. An operating manual including construction drawings is being prepared.

Circulation through the sodium purification system continued with the secondary sodium storage tank temperature maintained at 350°F. Minor system modifications were completed.

As reported in Progress Report for April 1963, ANL-6717, p. 16, the moisture and hydrogen content of the secondary piping system was being monitored to determine base values prior to filling the system with sodium. The moisture and hydrogen values were higher than expected, and the system was partially evacuated and purged with new argon (dew point of -95°F) to reduce these contaminants. Following filling, the dew point in the system was -40°F and the hydrogen content 180 ppm. The dew point and hydrogen content remained essentially constant during the following 18 days at ambient temperature.

Heatup of the system for sodium filling was started on May 13 and completed by May 15. During this period, the moisture content and hydro-gen content were rising rapidly. The temperature was maintained at 350°F. By May 18, the dew point had risen to +15°F and the hydrogen content to 1780 ppm. Following evacuation to about 23 in. Hg and refilling with dry argon, the dew point was -46°F and the hydrogen 500 ppm. Since that time, the temperature has remained at 350°F and the dew point has risen to -15°F while the hydrogen content has risen to 1900 ppm.

Efforts continued to determine the amount and origin of moisture and hydrogen in this system. Data are being obtained by means of a dew-point indicator, electrolytic hydrometer, gas chromatograph, and a mass

spectrometer. Meaningful conclusions cannot yet be drawn, since it is difficult to obtain representative samples from this system. Some of the data have also been misleading due to malfunctioning equipment.

The pressure on the water side was held at 1000 psig until May 25 and then was lowered to 500 psig. At month's end, the secondary sodium system, steam generator, and steam piping were being held at 375°F under isothermal conditions with 500 psig on the water side pending further tests in search of information on the source of moisture and hydrogen in the secondary sodium system. At this time, the data indicate the moisture and hydrogen could come from adsorbed moisture and hydrated oxides in the piping system. The most reasonable mechanism for the hydrogen formation is oxidation of the chrome-moly steel due to surface moisture and the resulting evolution of hydrogen.

Filling of the system is currently being delayed until the moisture and hydrogen can be reduced to an acceptable low level and until its presence can be explained.

3. Power Plant

A duplex strainer was installed in the condensate line leading to the desuperheater in the condenser, and the condensate pump was repacked. Color coding of the piping proceeded intermittently, and painting of the turbine-generator was started.

On May 13, the entire steam system was placed in operation, and the heat-up of steam generators prior to sodium filling was started. By noon of May 15 the systems were at filling temperature (350°F). However, the presence of hydrogen and moisture in the blanket gas of the secondary sodium system (see above) has postponed sodium filling.

The steam system has remained in operation, maintaining the steam generators at 350°F. No problems were encountered during the system startup.

4. Fuel Cycle Facility

After the installation of new refrigerant control valves in the Argon Cell cooling and pressure-control system, the valves were calibrated for delivery of refrigerant and the system retested. Satisfactory operation was obtained under simulated conditions of rapid changes of barometric pressure and heat load. Response of the automatic control instrumentation was adequate. The purification-system compressor was operated for prolonged periods in an isolated system to evaluate bearing lubrication.

The process off-gas system was completed and leak tested. The diaphragm valves were not seating satisfactorily and replacement of the Teflon seating rings will be necessary.

Low-melting alloy was melted and poured several times with one melt-refining furnace by remote techniques. A copper ingot was also poured, marking the first high-temperature operation. The first phase of technician instruction in the melt-refining operation was completed and will be followed by actual operating observation and practice.

An injection-casting charge table, pallet load-and-unload station, two pin-processing machines, and a fuel rod-assembly station were delivered to the EBR-II site. With the exception of one pin-processing machine, these were installed in the Argon Cell of the Fuel Cycle Facility (FCF). One pin-process machine was set up for operation in the FCF mockup area for training purposes. The data processor, used in conjunction with the pin-process machines, was tested and made operational. The controls for the pin-process machines were checked and found to require minor revisions.

Bronze was melted and cast in an injection-casting furnace. Some overheating was encountered and the graphite crucible cracked. Minor damage to the furnace parts has been repaired.

A pin-processing machine was placed in the Argon Cell for operational checkout of components. In one instance, a jam occurred in the demolding shear, but was successfully cleared after devising special tools. Checkout of data-processing machines is progressing.

5. <u>Detector for Fuel-element Failure</u>

A detector for delayed neutrons emitted by fission fragments in the sodium coolant of EBR-II has been under development. The program was previously reported in ANL-6658 (Monthly Progress Report for October 1962, p. 27). The output-information-processing unit for use with the EBR-II installation was re-evaluated and tentative specifications were worked out for a number of different systems. A thorough effort to obtain a bid from manufacturers of information-processing equipment on the basis of these specifications yielded no return. A suitable unit will therefore have to be assembled from purchased components.

Briefly, the problem to be solved was to record a very small count-rate excursion of possibly less than 1-sec duration. At the same time, a possible spike, several orders of magnitude larger, also must be recordable, in order to have at least some idea of the extent of damage in case of a partial meltdown. This problem can be readily solved by recording

the output of the fuel-element-failure detector on magnetic tape (which allows up to 10^3 cps random digital signals without difficulty) and transferring this information on demand to a fast chart recorder. Orders are now being placed for the required components.

Much of the detection equipment has been delivered. The electronic system is now on hand, except for one amplifier. Graphite has been machined to size, and various hardware items are being put together (the different parts of the detection unit have to fit rather well, since space inside the lead shield is very tight). A final check-out of the whole detection and signal-processing unit will be undertaken in the near future. The readout equipment, to be located in the EBR-II control room, is now being detailed from plans which were developed earlier.

The lead shield which surrounds the detector station was redesigned in order to provide limited accessibility to the detectors as well as space for the preamplifiers and necessary cooling. A calibration neutron source access hole will be provided.

6. Fuel Development

a. Fuel Jacket Development. Isochronal (2-hr) annealing studies were conducted on Nb-1 w/o Zr (the EBR-II Core II reference jacket material, mentioned in the March Progress Report, ANL-6705, p. 23), Nb-5 w/o Zr (D-14), Nb-10 w/o Ti-5 w/o Zr (D-36), and Nb-39 w/o V-1 w/o Ti in order to determine stress relieving and recrystallization temperatures. For the first three alloys, four rolling-deformation percentages were studied, whereas for the last only three were investigated.

The annealing was performed in vacuums less than 0.1 μ. The suggested stress-relieving and recrystallization temperatures, as shown in Table II, were determined from hardness measurements. In general the degree of deformation did not affect these temperatures.

Table II. Annealing Temperatures (°C) for Four Niobium Alloys

Alloy (w/o)	Stress Relieving	Recrystallization
Nb-1 Zr[a]	750-850	1150-1250
Nb-5 Zr (D-14)	600	1250
Nb-10 Ti-5 Zr (D-36)	-[b]	1100
Nb-39 V-1 Ti	600	1100

[a] The lower-temperature values correspond to the high-purity material in each case.

[b] The hardness values continuously dropped from room temperature to the recrystallization temperatures.

Small-button arc melts of several vanadium and niobium alloys have been made during the month. The buttons will be fabricated into coupons for test of corrosion in sodium and into specimens for other evaluation tests.

V-10 w/o Ti and Nb-5 w/o Mo alloys have been fabricated into required $\frac{1}{16}$-in. sheet stock. Scrap resulting from the fabrication of the Nb-5 w/o Mo at 1000°C was remelted and is to be rolled at a lower temperature, if possible, to provide samples with a different fabrication history.

Initial fabrication attempts with the Nb-39 w/o V-1 w/o Ti alloy proved unsuccessful. Further attempts will be made as soon as more alloy is cast. Alloys of V-20 w/o Ti and V-20 w/o Nb-5 w/o Ti are being prepared for fabrication.

b. Properties of Uranium-Plutonium-Fizzium. Two U-Pu-Fz alloys and one U-Pu-Fe alloy were studied for thermal-cycling stability. Injection-cast EBR-II-size pins of the composition shown in Table III were cycled 100 times between 475°C and 750°C. The specimens were held for one hour at 750°C and for 4 hr at 475°C, with transfer times of 15 min for heating and cooling. None of the alloys showed any significant changes in length or diameter.

Table III. Composition of Thermal-cycled Alloys, w/o

U	Pu	Fz	Fe
70	20	10	-
80	10	10	-
43.6	17.4	-	39

Transverse fracture tests have been conducted to determine the effect of composition and heat treatment on the ambient temperature strength of U-Pu alloys. The results of testing $\frac{5}{16}$-in.-diameter by $1\frac{3}{4}$-in.-long specimens in a three-point loading fixture are given in Table IV. Most of the values are an average of three or four tests. From these results it appears that the heat treatment has a very significant effect on strength. In all alloys, the heat-treated specimens had greater strength than as-injection-cast specimens. In the as-cast condition, the alloys in order of decreasing strength were U-10 w/o Pu, U-10 w/o Pu-10 w/o Fz, and U-20 w/o Pu-10 w/o Fz. In the homogenized condition it appears that the alloys in order of decreasing strength were U-10 w/o Pu-10 w/o Fz, U-20 w/o Pu-10 w/o Fz, and U-10 w/o Pu. The alloys U-10 w/o Pu-10 w/o Fz and U-20 w/o Pu-10 w/o Fz were oil quenched after the homogenization anneal for retention of high-temperature phases. The alloy U-10 w/o Pu was not quenched since the high-temperature phases cannot be retained. The U-10 w/o Pu-10 w/o Fz alloy was also tested after a heat treatment consisting of homogenization and a 450°C anneal for stabilization of low-temperature phases. As can be seen in Table IV, the strength after this heat treatment was slightly greater than the strength of the as-cast specimens of this composition.

Table IV. Effect of Composition and Heat Treatment on Ambient
Temperature Strength of Injection-cast U-Pu Alloys

Alloy Composition	Heat Treatment	Fracture Force (lb)	Maximum Stress at Fracture (psi)	Average Stress at Fracture (psi)
U-10 w/o Pu	As Cast	1062	119,800	60,960
U-10 w/o Pu-10 w/o Fz	As Cast	920	103,800	59,600
U-20 w/o Pu-10 w/o Fz	As Cast	575	64,900	33,000
U-10 w/o Pu	48 hr at 900°C, 2 hr at 450°C, Furnace Cool	1152	129,900	66,120
U-10 w/o Pu-10 w/o Fz	24 hr at 750°C, 144 hr at 800°C, 48 hr at 650°C, Oil Quench	1720	194,000	111,400
U-20 w/o Pu-10 w/o Fz	192 hr at 780°C, Oil Quench	1319	148,800	85,400
U-10 w/o Pu-10 w/o Fz	24 hr at 750°C, 144 hr at 800°C, 168 hr at 450°C, Furnace Cool	1050	118,400	60,300

Several creep tests of U-10 w/o Pu and U-10 w/o Pu-10 w/o Fz
alloys were made in a high temperature tensile and creep-testing machine.
Specimens were identical in size, shape, heat treatment, and fabrication
in the creep and tensile tests, that is, as injection-cast, $\frac{1}{4}$-in.-diameter,
1-in.-gauge length, cylindrically shaped, threaded-end specimens.
Differential-stress isothermal creep tests were conducted up to six days
in 10^{-5} torr vacuum to establish the stress dependences of the minimum
strain rate presented in Table V.

Table V. Stress Dependence of Minimum Strain Rate for U-10 w/o Pu and U-10 w/o Pu w/o Fz

Alloy	Temp (°C)	Strain Rate $\dot{\varepsilon}$ (in.-in.$^{-1}$-min^{-1}) in terms of stress σ (psi)	Testing Conditions		Fracture Strain ε_f (in.-in.$^{-1}$)
			Stress σ (psi)	Strain Rate $\dot{\varepsilon}$ (in.-in.$^{-1}$-min^{-1})	
U-10 w/o Pu	300	$3.63 \times 10^{-26} \sigma^{5.04}$	9,000-14,000	4×10^{-6}-3×10^{-5}	Specimen failed prematurely at macroscopic defect
U-10 w/o Pu	550	$7.83 \times 10^{-18} \sigma^{3.68} \pm 15\%$	3,500-7,500	1×10^{-4}-2×10^{-3}	0.015
U-10 w/o Pu-10 w/o Fz	409	$9.99 \times 10^{-7} \exp(3.51 \times 10^{-4}) \sigma \pm 15\%$	12,000-25,000	1×10^{-6}-5×10^{-5}	0.0288
U-10 w/o Pu-10 w/o Fz	551	$2.20 \times 10^{-7} \exp(8.45 \times 10^{-4}) \sigma \pm 8\%$	3,500-7,500	4×10^{-6}-2×10^{-4}	0.0185

The time for 1% creep at the surface of a 0.144-in.-diameter U-10 w/o Pu-10 w/o Fz pin at 550°C was calculated for second-stage behavior from thermal stresses and creep data. The time under the effective stress is unrealistically short, owing to neglect of stress relaxation. A method was therefore developed by which the time for 1% creep could be calculated through incorporation of the relaxation of stress. The actual time for 1% creep would lie between these extremes. The results of these calculations are given in Table VI. These values were obtained under the assumption that the power was generated within the specimen (as occurs in reactor fuels) so as to create a radial temperature gradient. A coolant is assumed to maintain a constant temperature at the surface of a specimen regardless of the power input.

Table VI. Time for 1% Creep at a Surface Temperature of 550°C with and without Stress Relaxation in a U-10 w/o Pu-10 w/o Fz 0.144-in.-diameter Fuel Pin

Power (w/cm^3)	ΔT (°C)	Effective Surface Stress (psi)	Time for 1% Creep under Effective Stress (hr)	Time for 1% Creep with Stress Relaxation (hr)
1735	50	6,300	3.5	Stress relaxed before 1% creep
4000	115	14,600	2.9×10^{-3}	3,350
5205	150	18,600	9.3×10^{-5}	106

A method has been devised for rolling 0.001-inch foil from the U-20 w/o Pu-10 w/o Fz alloy, which heretofore has been considered too brittle to permit rolling. Phase-relationship studies suggested that the brittleness can be attributed to low-temperature phases. Based on this lead and considerable perseverance, the following method was devised. A $\frac{1}{4}$-in.-thick casting was jacketed with a cold-rolled steel pack that was coated with alumina, and rolled in the temperature range 590-620°C. The pack was initially heated for $\frac{1}{2}$ hr at 640°C, then reheated for 7 min after each pass through the mill. Various jacket materials were tried, but none were as good as cold-rolled steel. Attempts to roll at a higher temperature caused alloying with the jacket. Below 590°C, the material was extremely brittle and shattered on rolling.

The alumina coating on the steel worked well down to 0.006 in., but below this thickness alloying took place in spite of the protective coating. A thin coating of Aquadag on the steel was found to prevent alloying and permitted rolling of the 0.006-in. foil to the final 0.001-in. size.

c.   Compatibility of Plutonium-bearing Fuels with Cladding Materials. Uranium-plutonium and uranium-plutonium-fizzium alloys are being tested for compatibility with potential refractory metal cladding as part of our study of fuel and clad materials for EBR-II, Mark II loading.

The fuel-clad combinations being studied are U-10 w/o Pu and U-20 w/o Pu-10 w/o Fz with niobium and U-10 w/o Pu-10 w/o Fz with niobium, Nb-1% Zr, molybdenum, and vanadium. These combinations are being studied by annealing diffusion couples at 550, 600, and 650°C for 7, 17, and 42 days.

Penetration (see Table VII) is taken as the total width of the diffusion band as seen metallographically. The interdiffusion bands in both the U-10 w/o Pu-10 w/o Fz vs. niobium and the U-20 w/o Pu-10 w/o Fz vs. niobium systems appeared to form almost 100% in the niobium. Total band widths in Table VII can therefore be taken as penetration into niobium. As can be seen from the data, U-20 w/o Pu-10 w/o Fz alloy is considerably more aggressive than U-10 w/o Pu-10 w/o Fz alloy. Penetration of the U-20 w/o Pu-10 w/o Fz alloy appears to be about double that of the U-10 w/o Pu-10 w/o Fz alloy.

Table VII. Width (mils) of Diffusion Bands
(All compositions in weight percent and vs. niobium)

Temp (°C)	7-day anneal		17-day anneal		42-day anneal	
	U-10 Pu-10 Fz	U-20 Pu-10 Fz	U-10 Pu-10 Fz	U-20 Pu-10 Fz	U-10 Pu-10 Fz	U-20 Pu-10 Fz
550	0.12	0.25	0.19	0.34	0.22	0.50
600	0.28	0.47	0.41	0.78	0.63	1.44
650	0.59	1.00	1.16	2.94	3.16	6.70

d. __Uranium-Molybdenum Alloys.__ Success in rolling U-14 w/o Mo at a temperature as low as 950°C (see April Progress Report, ANL-6717, p. 23) had been achieved to a total of 30% reduction. Further evaluation has shown that, although the alloy can be rolled to a 0.5-in.-diameter bar (about 80% total reduction) at 1000°C, it cracks on rolling to this diameter at a temperature of 950°C.

Attempts were made to extrude 0.725-in.-diameter x 1.75-in.-long U-14 w/o Mo specimens jacketed in a $\frac{1}{8}$-in.-thick Zircaloy-2 can. Although the alloy has been extruded at a temperature of 1000°C without cracks, the dogbone effect and irregular diameter of extrusion resulted from the Zircaloy-2 jacket being too soft in comparison with the U-Mo alloy at the temperature of extrusion. Lower extrusion temperatures are being investigated.

7. Remote Fabrication Development

Capacity-discharge welders are among the EBR-II equipment that has been designed, built, developed, and tested for performance. They are used for making closure welds on EBR-II fuel rods by discharging a bank of electrical capacitors across a gap formed between a tungsten electrode and the jacket-restrainer plug. The remote-controlled equipment which
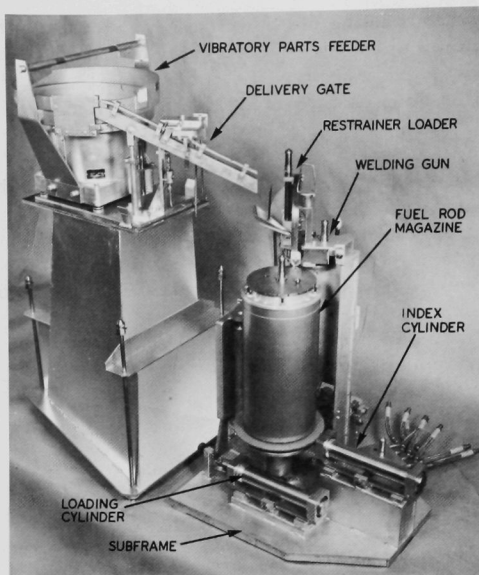
Figure 10. Restrainer Feeder and Welder

feeds the restrainer-plugs, inserts them into the loaded fuel tubes, and makes the closure welds is shown in Figure 10.

The restrainer feeder consists of a vibratory hopper which delivers restrainers to a pair of gravity-feed rails. A pneumatically actuated gate delivers these restrainers, one at a time, into the restrainer loader mounted on the welding machine. Fuel tubes are preloaded in a 20-rod rotary magazine which is placed upon a spindle in the welding machine and which swings into position below the restrainer loader and welding gun.

Indexing is accomplished by a rotary cam mechanism which successively positions each fuel tube below the restrainer loader and welding gun. The loader inserts the restrainers into the fuel tubes. The restrainer loader is selective. It will not release the restrainer unless a fuel tube is in position or unless the restrainer is seated against the shoulder of the tube, but will then retract it. The restrainer-loading feature was provided before sealed master-slave manipulators were available. Since these are now available, they will serve as an alternate means of restrainer loading.

The magazine is then indexed. The fuel rod is depressed by a cam as it is brought into position under the welding electrode establishing a 0.040-in. gap. Provision is made for clipping and repositioning the tungsten electrode. The welding gun is purged with helium and the capacitors are discharged by a programed controller.

The machine is designed for manipulator disassembly into the components shown in Figure 11. Considerable realignment of the components as received from the vendor was necessary before the machine would work properly. Several hundred welds have been made satisfactorily and the equipment has been shipped to Idaho for installation in the Fuel Cycle Facility.
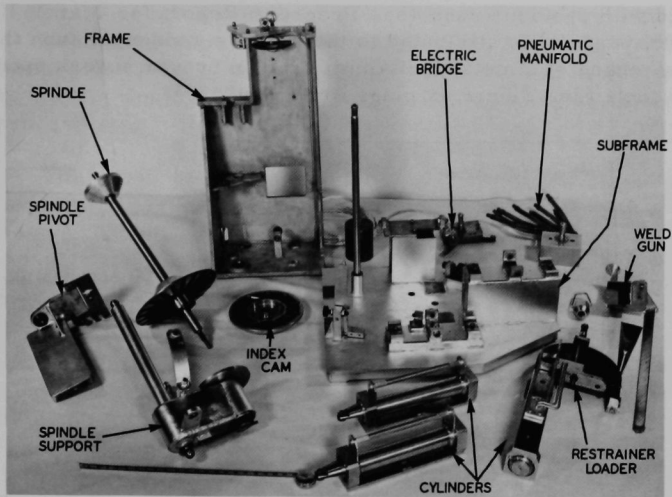
Figure 11. Welder Disassembly

8. Process Development

a. Melt-refining Process Technology. Two small-scale experiments were performed in order to investigate further the behavior of fission product iodine in the melt-refining process. Twenty-gram samples of uranium-5 w/o fissium alloy, containing cesium and either potassium iodide or cesium iodide with iodine-131 tracer added, were melt refined for one hour at 1400°C in a zirconia crucible contained in a closed, tantalum collector tube. In the experiment with potassium iodide (b.p., 1325°C), the iodine activity condensed in a temperature zone from 1400 to 350°C. In the case of cesium iodide (b.p., 1280°C), the activity was found in a zone between 790 and 1020°C. The latter result is in agreement with the iodine distribution observed previously with high-burnup fuel and is considered to be further support for the hypothesis that the fission product iodine which is volatilized during melt refining is primarily in the form of cesium iodide. The distribution of the iodine in the two experiments as a function of the temperature along the wall of the tantalum condenser is shown in Figure 12.

Within the accuracy of the experimental method, material balances of 100 percent were obtained. More than 99 percent of the iodine charged was found condensed on the tantalum condenser. A total of less than one percent of the iodine charged was found in the product ingot, skull material, and crucible. The much better material balances obtained as

compared with previous runs (see Progress Report for March 1963, ANL-6705, page 26) is attributed to the use of a condenser tube that was sealed by means of a metal (tantalum) cap. In previous work open tubes or tubes containing Fiberfrax plugs were used.
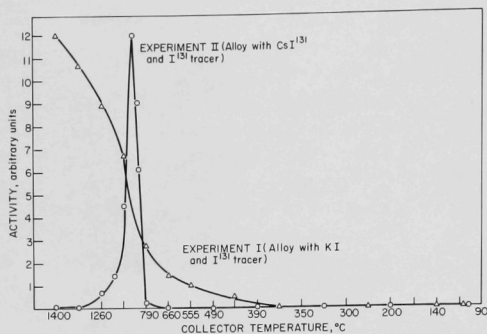
Figure 12

Iodine-131 Activity Collected in Tantalum Tubes Employed During Melt-refining Experiments

b.   Skull-reclamation Process. The purpose of the skull-reclamation process is the recovery and purification of the fissionable material contained in the crucible residue (skull) remaining after a melt-refining operation. Two laboratory-scale demonstration runs were completed during the past month.

In one run, the noble metal-extraction step consisted of heating at 650°C about 76 gm of skull material which had not been converted to an oxide powder in an agitated salt flux-metal system (calcium chloride-magnesium chloride-magnesium fluoride-zinc chloride flux phase; zinc metal phase). The objective was to oxidize uranium into the molten salt phase with zinc chloride, which was present in the salt at an appropriate concentration. The yield of uranium for the entire skull reclamation run was low (about 80 percent); the removal of cerium, zirconium, and molybdenum was very poor, whereas the removal of ruthenium was good. A large uranium loss was experienced when the waste supernatant was removed after the precipitation of the uranium-zinc intermetallic compound.

In a later run, which has not yet been completed, it was determined that this loss might have resulted from mild mechanical stirring during the precipitation of the intermetallic compound and transfer of the supernatant solution, thereby causing a small amount of precipitate to be suspended. Elimination of the stirring reduced uranium losses to near the expected value of one percent.

In the other completed run, carbon was added to the system during the uranium oxide-reduction step to augment the zirconium-removal capability of the skull-reclamation process through formation of zirconium

carbide and its removal in the waste salt. Removal of zirconium by this means was found to be slight and some uranium was lost, presumably through the precipitation of uranium carbide. It was concluded that the addition of carbon would be of little value in the removal of zirconium during this process step.

The use of partial rather than complete oxidation of skull material is a possible method of removing the skull from the melt refining crucible (see Progress Reports for January and March 1963, ANL-6683, page 16, and ANL-6705, page 27). The partial oxidation of the skull material was carried out while it was contained in an inverted crucible. It was necessary to oxidize about one-fourth of the skull before it fell free from the crucible. Since this considerable amount of oxide would have to be processed through the skull-reclamation process steps which follow oxidation, any advantages of partial oxidation would be offset. No further development of this procedure is planned.

A large-scale ($2\frac{1}{2}$ kg of uranium) demonstration run of the skull-reclamation process was carried out in a tungsten crucible for all process steps. A uranium-dissolution step was introduced to enable the removal of the uranium precipitate from the tungsten crucible as a 12 w/o solution of uranium in 12 w/o magnesium-zinc alloy. All steps except the uranium-removal step were carried out without difficulty. Because of inadequate agitation, the dissolution of uranium in the magnesium-zinc alloy was incomplete and resulted in an unsatisfactory removal of uranium. It is believed that nearly complete removals can be achieved by providing more efficient agitation. The use of a single crucible for all steps of the skull-reclamation step except that for final retorting appears feasible and has certain advantages, the most important of which is the elimination of an entire furnace unit.

A study is being made on a 20-gm uranium scale to determine whether the noble metal-extraction step can be adapted to the removal of uranium from cladding materials. In these experiments, sufficient zinc chloride is added to the magnesium chloride-calcium chloride-magnesium fluoride salt mixture to oxidize uranium and thereby provide for its extraction into the flux. Experiments have been completed with unclad uranium-5 percent fissium fuel pins (0.144 in. in diameter; 1 to $1\frac{1}{2}$ in. long) and pins clad with Type 304 stainless steel, niobium-1 percent zirconium, or with Hastelloy-X coated on the inside with tungsten. The pins were contacted with zinc-salt mixtures at 750°C for 3 or 4 hr. The fuel pins dissolved completely in each experiment; the stainless steel and niobium-zirconium cladding dissolved completely. The Hastelloy-X cladding dissolved partially. The kind of cladding material or its absence had no apparent effect on the rate of uranium dissolution.

The skull-reclamation process requires the heating and mixing of molten metal-salt systems at temperatures to about 800°C. Low-frequency (60-cycle) inductive mixing is being investigated, since its use would result in a simplification of the process equipment. Inductive mixing was used in two runs in which skull oxides were reduced. In both runs, 80 percent reductions of 2.6-kg skull-oxide charges in magnesium-zinc flux systems were achieved in 2 hr at 800°C.

The runs were carried out in graphite crucibles. It is believed that higher uranium reductions can be obtained by (1) use of tungsten crucibles, which would eliminate the loss of uranium by interaction of uranium with graphite to form insoluble uranium carbide, and (2) degassing the skull oxide prior to its addition to the crucible or adding it in small increments rather than in one batch to prevent foaming of the molten salt flux. A tungsten crucible will be used in future work.

c. Blanket-processing Studies. The pilot-scale distillation unit for studying retorting of magnesium-zinc-plutonium supernatant solution generated near the end of the blanket process has been used for four preliminary runs. In two of the runs, uranium and 50 w/o magnesium-zinc alloy were charged into the still pot; in the other two runs, cerium was added to the uranium-magnesium-zinc charge as a stand-in for plutonium. Evaporation rates for 10- to 15-kg charges at 750 to 780°C and 38 to 44 mm Hg have been between 1.5 and 2 kg/hr. Cerium entrainment in the distillate was slight. Only about 0.2 percent of the cerium originally present in the still pot was carried over by the distillate.

d. Plutonium-recovery Process. Experiments to determine the solubility of plutonium in calcium solutions containing 0 to 70 w/o zinc are being done. Analytical results obtained to date indicate that plutonium solubility is much higher than originally anticipated. For example, plutonium solubility in calcium containing about 39 weight percent zinc ranges from 0.05 to 1.1 w/o in the temperature range from 405 to 850°C. The lower solubilities previously obtained for plutonium in plutonium-uranium-calcium-zinc systems (e.g., 0.022 w/o in calcium-36 w/o zinc at 424°C) are now believed to reflect either coprecipitation or reaction of plutonium with uranium. The solubilities of plutonium are roughly 10^3 to 10^4 times greater than the corresponding uranium solubilities.

e. Materials and Equipment Evaluation. In order to take advantage of the good mechanical properties of porous coarse-grained crucibles (such as of Alundum), attempts have been made to seal the pores of these crucibles for containment of metal and salt systems by impregnating the inner surfaces with a slurry of low-melting oxides (see Progress Report for January 1963, ANL-6683, p. 17). Subsequent firing of the crucible fuses the oxides, thereby sealing the pores. The coatings did not prevent the diffusion of process materials into the crucibles. No further work on this technique is planned at this time.

A series of experiments is underway to determine the effect of small amounts of added impurities on the stability of uranium-containing zinc-magnesium solutions. The stability of a 3 w/o uranium-5 w/o magnesium-zinc solution in the presence of 0.05 w/o beryllium was studied at 800°C in a tungsten crucible. The concentration of uranium was found to be unchanged after $10\frac{1}{2}$ hr.

9. Training

The training program during May involved systems training for technicians assigned to reactor operations, initiation of a series of class-room and field sessions to update the supervisory personnel in plant systems, specialized electrical training for new technicians and staff, detailed planning of training specific to wet critical and approach to power operation, and training plans for newly hired technicians.

III. GENERAL REACTOR TECHNOLOGY

A. Applied Nuclear Physics

1. High-conversion Critical Experiment (Light Water-moderated)

The analysis of the buckling data taken in the 1.27-cm square and 1.27-cm triangular BORAX-V lattices and in the uniform, seven-eighths-loaded, and three-fourths-loaded 1.24-cm square, stainless steel Hi-C lattice, was completed, and the buckling data for the 1.24-cm square, aluminum Hi-C core was taken.

The radial asymptotic region of the 1.24-cm uniform square, stainless steel Hi-C lattice was established as that region from which data points could be used for flux fittings such that:

(1) both bare and cadmium-covered foil traverses give the same value of radial reflector savings,

(2) the radial reflector savings are independent of the fitting radius.

The data obtained in the 1.24-cm square, stainless steel Hi-C core indicate that the radial asymptotic region extends to a radius of about 21 cm, or to within 55% of the extrapolated zero of the radial flux distribution. The axial asymptotic region was found to extend from the core center to within 85% of the extrapolated zero of the axial flux distribution. It was also found that the data obtained from cadmium-covered foils could be used for fitting even when containing points out to within 3 cm of the core boundary.

Table VIII gives the results of the buckling measurements. Only those data points in the asymptotic region of a core were used in flux

Table VIII. Buckling Measurements on the Hi-C and BORAX-V Critical Assemblies

Core	Radial Reflector Savings, cm	Clean Critical Radius, cm	Extrapolated Radius, cm	Radial Buckling, cm^{-2} $\times 10^4$	Axial Reflector Savings, cm	Extrapolated Height, cm	Axial Buckling, cm^{-2} $\times 10^4$	Buckling, cm^{-2} $\times 10^4$
				Results of Buckling Measurements				
uniform 1.24 cm square, SS Hi-C	7.69 ± 0.08 (18*)	29.40 ± 0.09	37.09 ± 0.12	42.04 ± 0.27	12.89 ± 0.27 (4)	134.81 ± 0.27	5.43 ± 0.02	47.47 ± 0.27
7/8 loading 1.24 cm square, SS Hi-C	7.26 ± 0.11 (1)	24.73 ± 0.02	31.99 ± 0.11	56.52 ± 0.39	12.38 ± 0.45 (1)	134.30 ± 0.45	5.47 ± 0.04	61.99 ± 0.39
3/4 loading 1.24 cm square, SS Hi-C	6.58 ± 0.06 (6)	22.40 ± 0.02	28.98 ± 0.06	68.87 ± 0.29	13.28 ± 0.49 (1)	135.20 ± 0.49	5.40 ± 0.04	74.27 ± 0.29
1.27 cm square, BORAX-V	7.35 ± 0.27 (4)	18.18 ± 0.05	25.53 ± 0.27	88.74 ± 1.89	11.32 ± 0.50 (1)	72.28 ± 0.50	18.89 ± 0.26	107.63 ± 1.90
1.27 cm triangular, BORAX-V	7.55 ± 0.10 (5)	20.74 ± 0.06	28.29 ± 0.12	72.27 ± 0.62	10.75 ± 0.50 (2)	71.70 ± 0.50	19.20 ± 0.27	91.47 ± 0.68

*Numbers in parentheses indicate number of independent determinations.

fittings of bare-foil data. Cadmium-covered foil data were used with points within 3 cm of the core boundary.

The error given for the buckling is a reflection of the uncertainty in the number of fuel rods required for criticality and the error in the reflector savings. The error given for the reflector savings is the standard deviation from the mean. In those lattices in which an insufficient number of measurements were performed to compute a meaningful standard deviation, the error for the reflector savings was estimated from the error obtained from similar lattices and the estimated error in the flux traverses.

The initial loading of the aluminum-clad fuel in the 1.24-square lattice was completed, and a relatively clean core was obtained for the flux traverse work. Due to increased finger-type rod worth, it was possible to move these rods completely to the core-reflector interface. The buckling data for this core have been taken, but the data reduction has not been completed.

Design and construction of a laminated foil holder containing cadmium, lead, aluminum, and uranium was completed. The holder was constructed to accommodate uranium foils irradiated in the Hi-C fuel and is designed to accomplish two purposes:

(1) to reduce the effects of backscatter between the upper and lower crystals, with particular reference to reducing the magnitude of the 100-kev fission product coincidence correction required in evaluating the U^{238} capture rates;

(2) to eliminate possible differences in overall detection efficiency between foils with different spatial distributions of U^{238} capture.

Results of experiments designed to determine the efficiency of the foil holder in accomplishing these objectives are now being evaluated. It appears that about a 15% reduction in the fission product gamma-ray contribution to the coincidence count rate is achieved.

2. Preparations for Plutonium Criticals

Planning is proceeding for a program of plutonium-fueled, light water critical experiments which may be performed in ZPR-VII. A careful review of the published literature on plutonium-fueled thermal systems has been made and program objectives are being more clearly established.

Survey calculations aimed at outlining the fuel requirements are in progress. The reactivities and critical masses of a series of PuO_2-natural UO_2-fueled lattices have been calculated to give quantitative information on the variation of these quantities with plutonium isotopic composition, enrichment, and hydrogen-to-heavy atom ratio.

3. Theoretical Physics

   a.   ZPR-VII Data Analysis. A version of U^{235} having resonance absorption and fission parameters has been added to the GAM-1 library. The resonance parameters were taken from GA-2151,[2] which is the report describing how the smooth absorption and fission cross sections for the old U^{235} GAM-1 isotope were obtained. Straightforward use of the resonance parameters in the Adler-Hinman-Nordheim resonance integral formulation of GAM-1 would lead to too much absorption and not enough fission in the resonance region. Thus, a scheme was devised wherein the calculated resonance absorption and fission integrals are multiplied by a constant (~ 0.837) which was chosen so that the resulting infinite dilution resonance absorption and fission combined with some smooth absorption and fission with a value of $\alpha = 0.174$ gives the old GAM-1 smooth absorption and fission integrals in the resonance region. The necessity for using a scheme other than the straightforward use of Breit-Wigner single-level parameters arises because a multilevel formulation is needed for accurate description of resonance fission. The scheme used here should give a reasonable estimate of U^{235} self-shielding effects, without greatly complicating the analysis.

   The revision of the Fortran codes (1512/RE) used for calculating cadmium cutoff values and foil activations, which was mentioned in ANL-6705 (Progress Report for March 1963, p. 38), is nearly complete. Outputs of sample problems have been spotchecked with desk computer calculated values.

B.   Reactor Fuels and Materials Development

1. Ceramic Fuels

   a.   Uranium-Plutonium Carbide Fuel. Four reaction melts of (U,Pu)C were made, but so far only two of them have been analyzed for carbon. The carbon content of the first melt was in the range from 3.4 to 3.8 w/o, and that of the second melt was 4.6 w/o, which is slightly below the stoichiometric value.

   A single vibratory-compacted specimen of PuC containing 6.22 w/o C and compacted to 80% of theoretical density was irradiated in the CP-5 reactor to a calculated burnup of 5.3% of the metal atoms at a maximum cladding surface temperature of 570°C. The specimen is an EBR-II-type pin with a 0.176-in. OD and 0.009-in., Type 304 stainless steel cladding with a 2-in.-long fuel section in $3\frac{1}{4}$-in. overall length. Thermocouples at six positions near the specimen indicated satisfactory performance during the irradiation period. When the capsule was autoradiographed at the end of the experiment, however, the specimen was

---

[2] A. J. Goodjohn and N. F. Wikner, Suggested Values for the Partial Cross Sections of U^{235} for Use in the Neutronic Analysis of Thermal and Intermediate Reactors, GA-2151 (July 1961).

found to be ruptured and fuel was disseminated about the tantalum retaining cup. The exact occurrence of failure could not be determined from the thermocouple data. Postirradiation examination of this specimen will begin shortly.

A temperature-controlled capsule containing two vibratory-compacted specimens of PuC and four vibratory-compacted specimens of UC-20 w/o PuC in both Type 304 stainless steel and Nb-1 w/o Zr cladding has also been under irradiation in the CP-5 reactor. The specimens have the EBR-II geometry with a 2-in.-long fuel section. The fuel is compacted to approximately 80% of theoretical density. A thermocouple is adjacent to the cladding surface at the midplane of each specimen. Specimen temperatures, heat generation, and burnup are determined from the thermocouple data.

After approximately 1% burnup of the metal atoms at cladding surface temperatures ranging from 380°C to 625°C, the capsule was removed from the reactor and a pinhole autoradiograph made of the specimens. All were shown to be intact. The capsule was reinserted in CP-5 and achieved burnups ranging up to approximately 2.2% of the metal atoms. The capsule was again removed from the reactor; neutron radiographs indicated that all specimens were intact. The capsule has been reinserted in the reactor for further irradiation.

A temperature-controlled capsule containing specimens identical with those in CP-5 has been shipped to the MTR for irradiation. This is a gas-annulus capsule with a thermocouple adjacent to each specimen. These specimens are scheduled to be irradiated at a cladding surface temperature of 600°C to 5% burnup of the metal atoms.

b. Uranium-Thorium Sulfide. Uranium monosulfide was prepared on a 100-gm scale by the reaction of finely divided uranium metal with a stoichiometric quantity of hydrogen sulfide at 500°C, followed by sintering in vacuum at 1900°C for 2 hr. It has been found that impurities present in hydrogen sulfide, such as nitrogen, carbon monoxide, and carbon dioxide, can be removed by pumping on the hydrogen sulfide while it is contained in a liquid nitrogen cold trap. A run using hydrogen sulfide purified by this method has been completed. Preliminary results indicate that the product had an insolubles content of 0.03 percent. The lattice parameter of the product (face-centered cubic, NaCl type) was found to be 5.490 Å (compared with a reported lattice parameter of 5.4903 Å[3]). Analysis of the product for oxygen indicated that more oxygen was present than could be accounted for by the insolubles. This suggests that oxygen may be in solid solution.

During the slow oxidation of US in air at temperatures increasing from 120 to 750°C, weight-change data, X-ray measurements, and visual observations were made. They indicate the following general behavior.

---

[3] E. D. Cater, P. W. Gilles, and R. J. Thorn, J. Chem. Phys. 35, 608 (1961).

Oxygen is taken into the NaCl structure of US interstitially, as is evidenced by the change in the line intensities of the powder patterns, to a considerable degree without changing the cell size. At a certain oxygen content, however, more oxygen causes the cell to shrink and the UO_2 fluorite structure is indicated. Although some of the sulfur content has been lost at this point, as high as perhaps 0.6 mole of sulfur is retained interstitially for each mole of UO_2. This sulfur persists in the structure as the UO_2 was further oxidized to U_3O_8, starting at about 350°C. Finally, at 700°C, the sulfur leaves the structure in an unknown manner and pure U_3O_8 remains, giving a good sharp pattern for the first time. This final sulfur loss corresponds to the previously unexplainable endothermic peak always encountered at about 735°C while oxidizing US in the differential thermal analysis (DTA) apparatus. The compound UOS seemed to form only extremely slowly at temperatures below 200°C.

Since early weighings were made before thermal equilibrium was attained, the compositions given are not necessarily exact.

As a preliminary investigation, six specimens of pressed and sintered uranium sulfide pellets clad with 0.012-in. Nb-1 w/o Zr alloy with a 0.002-in. helium annulus were irradiated in the MTR. The specimens were 0.281 in. in diameter and 3 in. in length, with a 2-in.-long fuel section and a $\frac{1}{2}$-in.-long gas space above the fuel. The pellets were either 80 or 90% of theoretical density. Three specimens contained annular pellets having a 0.080-in.-diameter axial hole the entire length of the fuel section.

The specimens were irradiated in NaK capsules over a range of calculated cladding surface temperatures from 310 to 630°C at cladding surface heat fluxes from 125 to 280 w/cm². Aluminum-cobalt flux monitors indicated a burnup range from 0.8 to 2.6% metal atoms. The flux determination will be confirmed by a mass spectrometric analysis of the uranium isotopes. The preliminary monitor-indicated data are given in the accompanying Table IX. Center fuel temperatures were calculated on the basis of a 0.001-in. helium annulus at temperature and a constant fuel thermal conductivity of 0.03 cal/(sec)(cm)(°C).

One specimen, S-5, had a circumferential bulge in the cladding at the intersection of the top pellet and the gas space. A pinhole autoradiograph of this specimen indicated a possible reaction between the sulfide pellet and the helical tantalum spring used to maintain the gas space in all specimens. The bulge accounted for a 0.008-in.-diameter increase in this region. No other specimen showed a diameter increase larger than 0.001 in. in the fuel zone.

Table IX. Preliminary Data on the Irradiation of Uranium Sulfide

Specimen No.	Configu- ration	% Theoretical Density	Indicated Burnup, a/o Metal	Cladding Surface Heat Flux, w/cm^2	Calculated Temperatures, °C	
					Cladding Surface	Fuel* Center
S-1	Solid	90	0.8	153	350	1460
S-2	Solid	90	2.0	238	550	2290
S-3	Cored	90	1.2	125	310	1200
S-4	Cored	90	2.6	280	630	2610
S-5	Solid	80	1.9	225	520	2170
S-6	Cored	80	2.0	205	480	1930

*Assuming a 0.001-in. annulus of helium.

The specimens will be punctured for fission gas measurement and then sectioned for metallographic and chemical studies. Further irradiations of uranium sulfide are in preparation with objectives of attaining cladding surface temperatures to 1000°C and burnups to 15% of the metal atoms. These irradiations will be performed in temperature-controlled capsules with at least one specimen containing a central thermocouple.

Measurements of the thermal conductivity of uranium-monosulfide have continued. The data are listed in Table X. The trend is now definitely toward increasing conductivity with temperature. The values from 0 to 500°C may be considered firm, but the values from 500°C to 1000°C are still preliminary. Measurements are continuing to 1000°C if possible.

Table X. Thermal Conductivity of Uranium Monosulfide

Temp, °C	k, cal/(sec)(cm)(°C)	Temp, °C	k, cal/(sec)(cm)(°C)
0[1]	0.0258	600	0.0352
100[1]	0.0273	700	0.0374
200	0.0286	800	0.0400
300	0.0299	900[1]	0.0421
400	0.0312	1000[1]	0.0445
500	0.0331		

[1]Extrapolated

c. Uranium, Thorium, Plutonium Phosphide. Synthesis of uranium monophosphide by means of the phosphine reaction has been investigated further. Additional experiments confirm that the best product is obtained when phosphine is reacted with uranium in the temperature range 300-400°C. Below this temperature range uranium hydride was observed

in the as-made material, and above this range UC was detected. The latter presumably forms by the reaction of uranium with CH_4, which is present in small quantities in the PH_3 gas. Particle size of the UP appears to vary with reaction temperature, despite the fact that all material received the same subsequent calcining treatment (at 1400°C). Material reacted at 700°C shows a 3.8-μ average particle size after calcining, material made at 500°C a 2.7-μ average size, and material made at 350°C a 1.9-μ average size. This trend does not continue with material reacted at 250°C, which exhibits an average particle size of 2.7 μ after calcining. Reasons for this behavior will be sought in future experiments.

Decomposition of U_3P_4 into UP and P occurs below 1200°C in vacuum. Preliminary evidence suggests that decomposition reaches a peak in the temperature range 1000-1100°C.

Initial electrical resistivity measurements of UP yield a room-temperature value of 250 microhm-cm.

Preliminary studies, involving measurements with a mass spectrometer, have been conducted on the vaporization of UP containing about 1% oxygen. Uranium monoxide and some UO_2 were the major gaseous species released between 1500 and 2000°C. Above 2000°C, the oxide gases diminished, and uranium and phosphorus gases became very prominent. These results corroborate weight loss data on UP, which indicate that weight losses first become significant above 2000°C. Metallographic analysis of the residue still showed fair amounts of UO_2, but only in the interior portions of the sample. Near the surface, the UO_2 had preferentially vaporized, leaving a relatively pure UP skin.

Single crystals of UP grew along the sides of the crucibles during heating of the samples above 2200°C. The crystals exhibit an average size of 0.2 mm and, based on single-crystal studies, are of good quality. Initially, it is planned to subject them to various irradiation doses in the CP-5 reactor to gain information on their irradiation behavior.

Further experiments were conducted on the sintering characteristics of UP powder; fabrication pressure and firing temperature were varied. Increasing the forming pressure from 20,000 to 40,000 psi resulted in an increase in fired density of from 3 to 5% at all sintering temperatures investigated. The sintered density versus temperature curves show a discontinuity between 1700 and 1800°C. The curve steepens considerably in this range, again becoming more gentle at higher sintering temperatures. Densities of the order of 92-93% of theoretical were achieved through use of forming pressures of 40,000 psi and through sintering at 2000°C for one hour. No increase in density occurs when sintering is carried out above 2000°C, since further shrinkage is offset by vaporization losses.

2. Irradiation Studies

a. <u>Swelling Studies</u>. A study is being made to determine if irradiation swelling of metal fuel can be improved by encouraging fission gas atoms to diffuse to free surfaces rather than agglomerating to form gas bubbles. One type of irradiation specimen designed to achieve conditions of minimum diffusion distance and good radial thermal conductivity consists of stacked thin disks of fuel. A central void is included to aid in venting fission gases.

The fuel samples were made from thin disks, 0.152 in. in OD by 0.056 in. ID, stacked to a height of one inch and encapsulated in a Nb-1 w/o Zr jacket. Two thicknesses of disks were used, 0.001 in. and 0.006 in., and three different clad designs were used, closed clad, vented clad, and unrestrained clad (open cage).

The first samples were fabricated from 20% enriched uranium. Some of these have been irradiated at a temperature and burnup which would normally result in swelling. They are now ready for postirradiation examination. Some U-20 w/o Pu-10 w/o Fz alloy has also been rolled into 0.006-in. and 0.001-in. foils, and similar disks made (see Section II.C.6). These are now ready to be encapsulated.

b. <u>Radiation Damage in Steel</u>

(i) <u>Radiation Damage Unit (RDU)</u>. A primary goal of this work has been to develop a measure of exposure for use in radiation-damage studies. In earlier work,[4] the vacancy-production cross section $[\sigma_v(E)]$ was introduced to give the average number of iron lattice atoms that a neutron of energy E could displace, assuming that the number of displacements would be proportional to the neutron energy and the scattering cross section of iron for neutrons of that energy. The resulting number of displacements was calculated on the basis that 25 ev were required to knock an atom out of its lattice site.

For neutrons having a fission spectrum distribution, the average displacement-production rate is 1350 per neutron/(cm²)(sec). Dividing the values of $\sigma_v(E)$ by 1350 gives a multigroup set of cross sections which, if multiplied by the multigroup values of the fission spectrum, gives unity. One neutron with a fission spectrum energy distribution is said to deliver one Radiation Damage Unit (RDU) in iron. The RDU is given as a function energy in the last column of Table XI.

In this work the spectrum is calculated by multigroup reactor theory. The activation rate for the reaction $Fe^{54}(n,p)Mn^{54}$ is calculated

---

[4] A. D. Rossin, <u>Radiation Damage in Steel: Consideration Involving the Effect of Neutron Spectra</u>, Nuclear Sci. and Eng. <u>9</u>, 137-147 (1961).

by means of the cross sections in Table XI. Since normalization of calculated spectra to absolute magnitudes of flux based on reactor power is subject to appreciable uncertainty, the spectrum is normalized by comparing the calculated activity of Mn^{54} with actual measurements. Enough Fe^{54} is present in iron so that activity can be determined precisely by counting a small chip from an irradiated steel specimen. The normalized spectrum is then multiplied by RDU values to give an effective rate of damaging exposure to fast neutrons.

Table XI. Multigroup Cross Sections

Group, i	E_L, Mev	ϕ_f Fission Spectrum	$S^{32}(n,p)P^{32}$ σ, b	$Fe^{54}(n,p)Mn^{54}$ σ, b	Fe^{56}, RDU
1	7.788	0.0064	0.350	0.650	3.518
2	6.065	0.0168	0.335	0.600	3.344
3	4.724	0.0464	0.260	0.530	2.700
4	3.679	0.0681	0.245	0.375	1.974
5	2.865	0.0966	0.170	0.150	1.310
6	2.231	0.1140	0.075	0.075	1.094
7	1.738	0.1190	0.030	0.030	0.876
8	1.353	0.1120	0	0.005	0.861
9	1.054	0.0983	0	0	0.589
10	0.821	0.0821	0	0	0.490
11	0.639	0.0646	0		0.461
12	0.498	0.0501	0		0.461
13	0.388	0.0371	0		0.573
14	0.302	0.0276	0		0.367
15	0.235	0.0197	0		0.292
16	0.183	0.0143	0		0.276
17	0.143	0.0100	0		0.249
18	0.111	0.0071	0		0.215
19	0.086	0.0049	0		0.174
20	0.067	0.0035	0		0.133
$\sum \sigma_i \phi_i$		1.00	0.065	0.0915	1.00

(ii) Experimental Results. The impact data obtained from steel samples irradiated under three different conditions are shown in Figure 13. In each case a 2-ft-lb transition-temperature shift is plotted against the integrated power of the reactor during the time the samples were in pile. The irradiation locations, and hence the spectra and temperatures, are identical within each set of results.
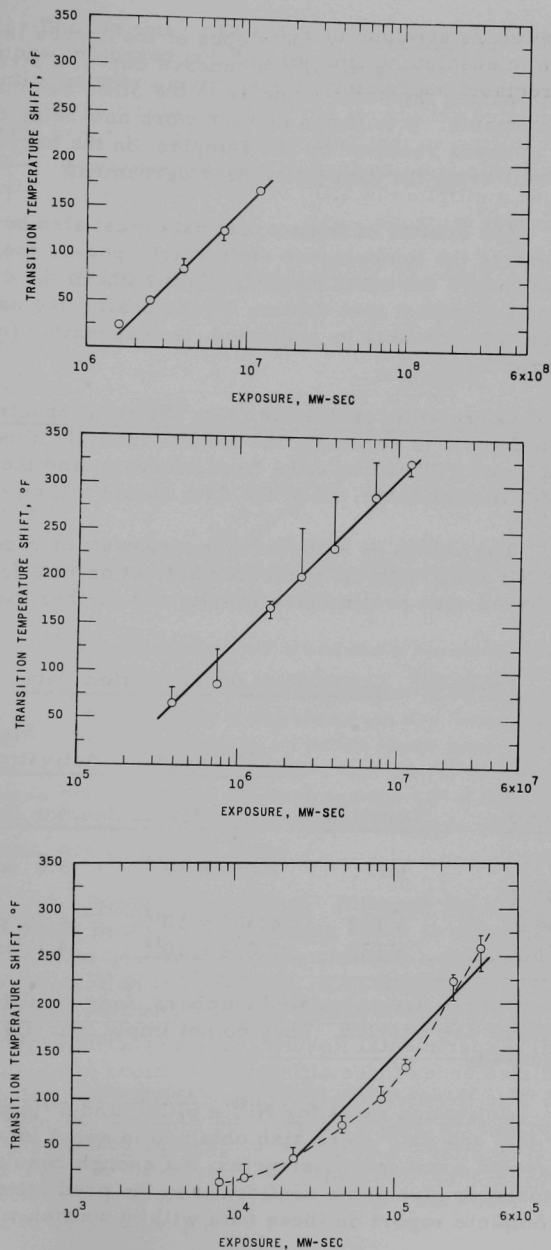
Figure 13. Results of Irradiations in Three Reactor Locations

The similarity in the slopes of the curves is evident. Even though the EBR-I data seems to form a concave curve, a straight line drawn through the data having the same slope as in the other two curves also appears to be reasonable. It is hoped that the work now being done on detailed determination of doses received by the samples, on the basis of induced Mn^{54} activity, will bring the data into closer agreement.

The scatter of impact test data must also be accounted for. The circles indicate the temperature shift which appears most reasonable. The error band covers the other possible places where the curve could be drawn, based on the impact test values. Occasionally, the use of only one odd datum point, which cannot be neglected, is responsible for the excessive width of the error band.

(iii) <u>Correlation of Results from Different Spectra.</u> The object of these irradiations is to reconcile the results from the three tests. If the determination of RDU values have been accurate, and the energy-dependent model is applicable, all of the data should fall on one line.

The values of RDU/sec per megawatt of reactor power are given in Table XII along with the measured activation rate for Mn^{54}. The Mn^{54} data are based upon preliminary results and further evaluations are necessary.

Table XII. Correlation of Irradiation Data

Reactor	Location	RDU/sec*	Mn^{54} Activations/sec
		per Mw of Reactor Power	
EBR-I	C17	1.016×10^{14}	5.6×10^{12}
CP-5 Fuel Element	VT14	6.583×10^{12}	4.13×10^{11}
CP-5 Dummy	VT22	7.074×10^{11}	4.17×10^{10}

*Since these are calculated numbers, four significant figures are carried. They do not imply four-figure accuracy.

Activation rates for $Ni^{58}(n,p)Co^{58}$ and $S^{32}(n,p)P^{32}$, and fission rates for U^{238} and Th^{232} were also obtained in some locations. Analysis of the data revealed some inconsistencies, but enough results were correlated satisfactorily to give some confidence to the predictions and cross sections. A complete report on these data will be written when the analysis is finished.

The Mw-sec values of the abscissae of three plots in Figure 13 are now multiplied by the appropriate RDU/sec. In Figure 14 the transition-temperature shifts are plotted against fast-neutron exposure in RDU.
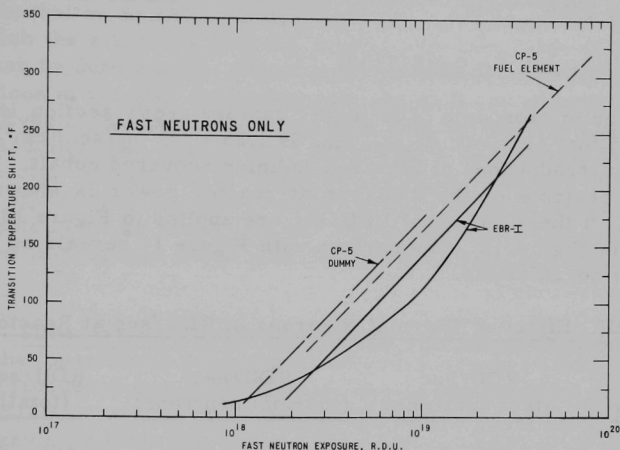

Figure 14. Transition Temperature Shift as a Function of Fast Neutron Exposure.

In this first attempt to reconcile these data some discrepancies were noted. Mn^{54} activity measurements are being made for all samples and the results may narrow or widen these gaps. The magnitude of the gaps are: about 30% between EBR-I and the CP-5 fuel element, and about 20% between the CP-5 fuel element and the CP-5 dummy. Four additional factors which may influence the size of the gaps, but are not included in the predictions, are discussed below.

(a) <u>Temperature Effect</u>. Although the irradiation temperatures are in a range in which no annealing effect is expected, if there were an effect at those temperatures the shift for a given dose would be less for higher irradiation temperature. The temperatures were: CP-5 dummy, 137°F; CP-5 fuel element, 148°F; and EBR-I, 275°F. This would tend to narrow the gaps.

(b) <u>Rate Effect</u>. At these temperatures, no appreciable effect is expected. However, if one existed, the samples receiving the lowest dose rate would be expected to show the greatest shift for a given total dose. The relative dose rates are about 1 to 9 to 140 for CP-5 dummy to CP-5 fuel element to EBR-I, respectively. An allowance for dose rate would tend to narrow the gap.

(c) <u>Thermal Neutrons</u>. Various models for the effect of thermal neutron contributions to damage have been proposed. Wechsler[5] computes the recoil energy of the nucleus as the capture gammas are ejected, and Harries <u>et al</u>.,[6] applying the formula to iron, comes up with about eight displacements per capture. To convert to RDU, we simply divided 8 by 1350. Thus

$$RDU(\phi_{th}) = \phi_{th}\sigma_{th}(8/1350) \quad .$$

For iron, the microscopic 2200-m/sec capture cross section is 2.53 b. In the CP-5 fuel element, $\phi_{2200 \, m/sec}$ is 1.25×10^{13} n/(sec)(cm^2), determined from irradiations of bare and cadmium-covered cobalt. The effect of thermal neutrons on the RDU/sec at reactor power is shown in Table XIII. If these values of RDU/sec are applied to Figure 13 the lines appear as in Figure 15. Comparison with Figure 14 reveals an improvement in the correlations.

Table XIII. <u>Effect of Thermal Neutrons in RDU/sec at Reactor Power</u>

Location	RDU/sec (fast neutrons)	RDU/sec (thermal neutrons)	RDU/sec (total)
EBR-I, C17	1.016×10^{14}	0	1.016×10^{14}
CP-5 Fuel Element	6.583×10^{12}	1.88×10^{11}	6.771×10^{12}
CP-5 Dummy	7.074×10^{11}	1.65×10^{11}	8.724×10^{11}
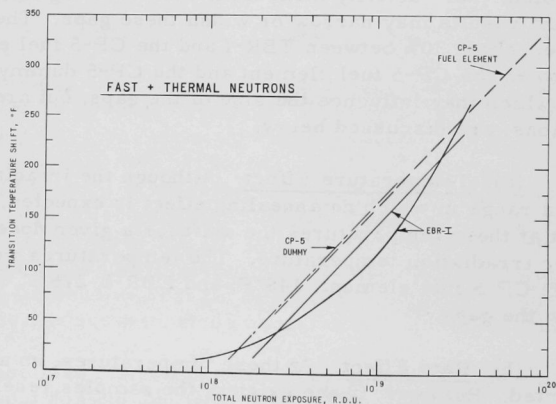
Figure 15. Transition—temperature Shift as a Function of Exposure to Fast plus Thermal Neutrons

[5]M. S. Wechsler, Fundamental Aspects of Radiation Effects on Diffusion-controlled Reactions in Alloys, ASTM 4th Pacific Area Conf., Los Angeles, California (October, 1962).

[6]D. R. Harries, P. J. Barton, and S. B. Wright, The Effects of Neutron Spectrum and Dose Rate on Radiation Hardening and Embrittlement in Steels, AERE-R4222 (Dec, 1962).

(d) The RDU contributions due to neutrons below 0.067 Mev are estimated to be: EBR-I ~+1%; CP-5 fuel element ~+3%; and CP-5 dummy ~+7%.

(iv) Detailed Dose Determination by Mn^{54} Activity. It was mentioned above that by counting the Mn^{54} activity in the region of a notch (the area in which the sample is broken), a more accurate value of fast-neutron exposure can be determined. Calculations have been made by means of the cross sections of the Mn^{54} activation rate and RDU per second throughout the core. Even if the DSN calculation fails to give true flux attenuation in the axial direction, the ratio of Mn^{54} activation to RDU should be consistently accurate. By counting a small steel sample from the broken surface of the Izod specimen, a measure of Mn^{54} activity in the material actually broken is obtained. By ratios, the corresponding RDU value is obtained. Work is now in progress to cut such chips from all of the irradiated material.

c. Time-Stress-Temperature Effects of SA-212B Steel. A 50% increase in the logarithmic decrement (internal friction) at the fundamental transverse frequency was found in sonic bars prepared from stressed EBWR SA-212B pressure vessel steel. These bars were prepared from a steel plug removed from the vessel for the fuel installation of a new 6-in.-diameter water nozzle when the EBWR facility was prepared for the 100-Mw power capability. The increase in internal friction along with a smaller one (10%) at the third harmonic frequency are ascribed to the combined effects of fabrication, stress history at temperature, and cold hydrostatic tests.

3. Development of Extrusion Techniques

Four extrusions have been made since the last reporting period (March Progress Report, ANL-6705, p. 46) by the modified DPM extrusion technique. The clad and central core materials were Type 304 stainless steel with an Al_2O_3-powder annulus. Two of the clad sleeves were made by drilling a solid rod. The other two sleeves were made with a full penetration weld along the full sleeve length. The composite billets were induction heated in air to 1150°C and extruded at a 5:1 reduction ratio through a 0.450-in.-diameter die with use of a 50-50 mixture of MoS_2 and graphite in oil as a lubricant. The same die, used in all four extrusions, showed a negligible amount of wash. The extruded surfaces were extremely good.

X-ray analysis, and transverse and longitudinal sections showed the extruded tubes to be of excellent quality. Sections of each tube were lightly swaged, and the central core and powder materials easily removed. Although the inner surfaces of the tubes were slightly roughened, they were fully acceptable for secondary fabrication without conditioning. Ultrasonic testing of the tubes revealed no apparent defects. However, the longitudinal

weld area did show up in the test. Two sections from each extrusion - one with the powder and core removed, and the other as-extruded with the core and powder annulus remaining - will be fabricated into small-diameter, thin-walled tubing and reinspected.

Hopefully, a welded sleeve can produce as good a finished tube as one using a seamless sleeve in extrusion. The technique will be applied to refractory metals and alloys by using a rolled and welded sleeve for billet make-up.

4. Corrosion Studies

a. Fuel-cladding Materials for Sodium-cooled Reactors. Wide variations with composition occur in the behavior of niobium-base alloys when exposed for 7 days to flowing sodium ($\sim \frac{1}{2}$ fps) at 650°C that has an abnormally high oxygen content. This conclusion was drawn from the results of tests (see Table XIV) with three niobium-base alloys in flowing sodium with an oxygen content estimated at a minimum of 200 ppm or even higher (because of suspected leakage of air into the test system).

Table XIV. Behavior of Niobium Alloys in Sodium

Sample	$\Delta w/A$, mg/cm^2**	Δ Thickness, mils**
Nb-39 w/o V-1 w/o Ti (1)*	-21.8	-1.2
Nb-39 w/o V-1 w/o Ti (2)*	-13.7	-0.94
Nb-1 w/o Zr†	-85.1	-7.14
Nb-5 w/o Zr†	-51.4	-2.64

*Supplied by Armour Research Foundation
**As removed from test and cleaned of sodium with
 alcohol and water, followed by ultrasonic cleaning.
†Commercial material

The Nb-39 w/o V-1 w/o Ti samples had adherent oxide coatings which remained after ultrasonic cleaning. The oxide layers on the Nb-1 w/o Zr and Nb-5 w/o Zr specimens were nonadherent. The edges of the Nb-5 w/o Zr sample were split open in a laminar fashion.

These results were obtained despite the presence of zirconium gettering chips in the sodium.

b. Structural Materials in Superheated Steam. Currently, four high-nickel alloys and a cobalt-containing alloy (René 41) are being exposed to steam at 650°C and 600 psi, flowing at 200 ft/sec. The oxygen

content of the steam is 30 ppm. The samples, examined after about 42 days exposure, appeared in good condition. Average metal penetrations varied from about 0.05 to 0.15 mils. INCO 625 and René 41 appear to be the better alloys in the group.

As part of a continuing effort to find alternative materials for superheat fuel cladding, Types 405 (12 w/o Cr, 0.2 w/o Al, balance iron) and modified 410 (12 w/o Cr, 0.5 w/o Ti, 0.5 w/o Si) stainless steels were corrosion tested in oxygenated steam at 650°C and 600 psi. Neither material appeared promising enough to warrant consideration for this application.

 c. <u>Aluminum Powder Products</u>. Powder products made at Trefimetaux (France) are being corrosion tested at 290°C in water containing about 30 ppm oxygen. Four samples were removed at 189 days and destructively defilmed. Average penetration of the metal was 1.3 to 1.6 mils. Visual observation indicated very little or none of the selective edge attack previously noted with powder products.

 d. <u>TD Nickel.</u> Water corrosion tests of bar samples of TD and commercially pure nickel have been continued. The exposure time now totals 83 days in degassed, distilled water at 360°C. The TD nickel has a cumulative weight gain of 0.354 mg/cm^2, compared with 0.299 mg/cm^2 for the commercially pure material. A few small protuberances developed on the abraded faces of the TD nickel sample, and many crystal-like particles were observed, at 50-diameter magnification, on the outer circumference of the sample. No such formations were observed on the commercially pure nickel.

 e. <u>Ceramics.</u> Pressed and sintered pellets of pure UO_2 and UO_2 containing 3 w/o additions of Gd_2O_3, Dy_2O_3, Sm_2O_3, or Eu_2O_3 have been corrosion tested in 650°C, 600-psi, refreshed, oxygenated steam for a total of 10 days and in 360°C distilled water for six days. Water exposures were conducted under both oxygenated and degassed conditions. There were marked differences in corrosion behavior among the various formulations, as shown below. All samples were of disc form, measuring about 0.64 cm high by 0.86 cm diameter.

In the steam test, the samples were relatively resistant during the first few days; no disintegration or cracking was observed on removal at 2.7 days. However, oxygen uptake was appreciable during this time. The oxygen concentration of about 30 ppm in the influent steam was reduced to less than 10 ppm in the effluent at the beginning of the test, gradually rising to 18 ppm after 10 days. The condition of the samples after 10 days was as follows:

Wholly or largely disintegrated (order of decreasing resistance)	Intact except for minor spalling (order of decreasing resistance)
	Eu_2O_3 edge cracking
Gd_2O_3	Sm_2O_3 scattered cracking and swelling
Dy_2O_3	UO_2 severe cracking and swelling

f. Light Alloy Suitable for Use with Mercury at Elevated Temperatures. In a continuation of a study of the effects of additives on the corrosion behavior of liquid metals, the presence of aluminum was found to inhibit the attack of mercury at 538°C on titanium. At this temperature, aluminum is appreciably soluble in mercury, yet a powdery gray scum, presumably either a mercury-aluminum amalgam or aluminum oxide, is formed. The weight gain of the titanium is small.

It was previously indicated that a saturated solution of nickel in mercury also results in inhibition of the corrosion of titanium at this temperature. However, no scum was observed in the case of the nickel addition.

Test results for 14-day static exposures are shown in Table XV.

Table XV. Interaction of Crystal Bar Titanium, Aluminum, and Nickel Exposed to Liquid Mercury at 538°C

Test Conditions	Weight Change, after 14 days mg/cm²	Spectrochemical Analysis of Exposed Surfaces*		
		Hg	Al	Ni
Liquid Mercury	-17.60	W	-	-
Liquid Mercury + Al (750 ppm)	+0.256	M	S-VS	-
	+0.316	M	S-VS	-
Liquid Mercury + Ni (750 ppm)	+4.04	M	-	M
	+3.92	M	-	M
Liquid Mercury + Ni (750 ppm) + Al (50 ppm)	-28.56	M	W-M	W-M
	-29.89	M-S	W-M	W-M

*VS - Very strong, 100% to 10% M - Moderate, 1% to 0.1%
 S - Strong, 10% to 1% W - Weak, 0.1% to 0.01%

Metallographic examination confirmed the weight change data, indicating no significant attack on the surfaces of titanium exposed in mercury containing either nickel or aluminum. It also confirmed that a small quantity of aluminum (50 ppm) added to a saturated solution of nickel in mercury accelerated the corrosion at this temperature.

This phenomenon of the interaction between additives in a confined system may be of theoretical interest in this general area.

5. Fuel-jacket Development for High-temperature Applications

Isochronal (2-hr) annealing studies were performed with two tantalum alloys: Ta-8 w/o W-2 w/o Hf and Ta-10 w/o W, under vacuums of 0.1 μ or less. The purpose of the study was to determine their approximate stress-relieving and recrystallization temperatures for various deformation percentages. These percentages obtained by cold rolling were approximately 20, 40, 60, and 80 percent. The two annealing temperatures, for each alloy, as shown in Table XVI, were determined from hardness measurements.

Table XVI. Annealing Temperatures (°C) for Two Tantalum Alloys

Alloy (w/o)	Stress-relieving	Recrystallization
Ta-8 W-2 Hf	650 (20 and 40% reductions)	1400 (60 and 80% reductions)
	850 (60 and 80%)	1500 (20 and 40%)
Ta-10 W	950	1600

The Ta-8 w/o W-2 w/o Hf annealing temperatures appeared to be more deformation dependent than the Ta-10 w/o W alloy.

C. Reactor Components Development

1. Viewing Systems

The innermost thick glass casting of a shielding window is quite susceptible to fracture during or after exposure to gamma radiation, if the glass is chipped or stressed in some other manner. The internal electric discharge results in a characteristic "tree-like" or dendritic fracture observed in the electrical breakdown of other transparent insulating materials. Since 1957, there have been five such discharges reported in this country and Japan. A study is in progress to determine the susceptibility to electrical breakdown of commonly used shielding

glasses. It is planned to expand the study to obtain a better understanding of the properties of the glass and the environmental conditions which contribute to breakdown.

The absorption of gamma radiation by the glass generates secondary electrons which produce a considerable charge separation within the glass. This charge separation results in an appreciable voltage gradient from the interior to the surfaces of a large block of glass. The means by which this charge separation is maintained is not known. However, it has been observed that the glasses having a particularly high volume resistivity, greater than about 10^{16} ohms-cm, are susceptible to electrical breakdown.

A lead silicate glass (3.3 gm/cm^3) currently used in shielding windows has been tested. A 4-in. cube of this glass has been discharged after only one-megaroentgen exposure at 35°C by mechanically fracturing the surface. The surface is fractured to a depth of about one millimeter by dropping a pointed probe. As the radiation exposure increases, the size of the dendritic fracture increases until it fills the entire block, except for a 1- to 2-cm-thick layer on all surfaces. The flash of light accompanying the discharge is shown in Figure 16.
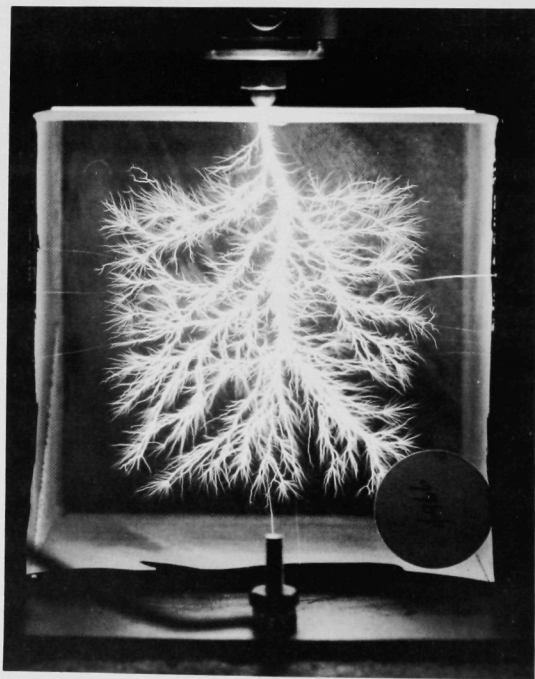

Figure 16. The Light Flash Generated When a 4-in. Cube of Lead Silicate Shielding Glass Undergoes Internal Electric Fracture Is Shown. The Pointed Probe at the Top Is Dropped to Trigger the Electric Breakdown. Exposure to Cobalt-60 Was 5.5×10^6 r at 1.4×10^5 r/hr.

It also has been observed that electrons are released from the interior of the block upon fracture, and a compensating charge flows to the outside of the block. The amount of charge released after a 10-megaroentgen exposure at 35°C is about 35 microcoulombs for a 4-in. cube for an exposure rate of 0.6×10^6 r/hr to Co^{60} gammas.

Increasing the temperature of irradiation reduces the fracture size and the charge released. For example, only a very small discharge (1.8 microcoulombs) occurred after a 10-megaroentgen exposure at 55°C. In addition, if the exposure of a constantly heated block is interrupted for 16 hr out of each 24-hour period, about the same size discharge (1.5 micro-coulombs) occurs for a 5°C lower temperature. This indicates that the exposure required to give a minimum discharge is more strongly influenced by temperature than continuity of exposure.

2. Electric Master-Slave Manipulator Mark E-4

This electrically connected master-slave manipulator will have some performance characteristics quite similar to the existing Electric Master-Slave Manipulator Model 3, but other characteristics will be markedly improved. The major characteristics of Mark E-4 are as follows:

1. The load capacity in any direction is 50 lb, the same as for Model 3.

2. The slave arm can be remotely repaired by a similar pair of manipulators, whereas the Model 3 can only be partially remotely repaired.

3. A more convenient arrangement for the master arm is provided over that of the Model 3.

4. The reliability should be better than that of the Model 3 and similar to that of the mechanical Model 8.

5. The dexterity will be somewhat better than that of the Model 3.

6. The manipulator is expected to cost 20 percent less to build than the Model 3.

7. The slave arm can be mounted on an overhead support system or on a vehicle to form a slave-robot.

A complete manipulator consists of a master arm, a slave arm, and a servo amplifier control system. The master arm and slave arm are similar. Each is composed of an upper arm and a lower arm. The design and detail work on the lower arms is nearly complete and parts are being fabricated. The design of the upper arms is approximately 50 percent complete.

Many of the parts of the servo drive units have been made. Each unit consists of four low-inertia servo motors, a gear train, a position transducer, and a brake. A breadboard model of an amplifier for these servo drive units has been made and is being tested.

It is expected that a complete experimental manipulator will be fabricated and under test by the end of this calendar year. This first design will be modified as indicated by its performance, reliability, and remote repairability.

D. Heat Engineering

1. Studies of Sodium Expulsion

The behavior of coolant during a fast reactor transient is being studied analytically and experimentally. A series of experiments are being designed with the goal of measuring accurately the transient pressure surge in a coolant following a large pulse of electrical power through a cylindrical resistor. The coolant will be contained in an annulus, the inner wall being the resistor, and the outer wall being quartz pipe so that photographic observations can be made.

An electronic triggering circuit based on a sequential firing of charged capacitors is being designed and instrumentation and structural materials are being purchased.

2. Studies of Boiling Metals

A small annular test section has been designed for performing sub-cooled and boiling burnout tests with sodium. Sodium is placed in the central tube which has a sprayed ceramic dielectric (insulation) on the outside. A nonreactive metal is placed in the annulus and is heated electrically. Procurement of this experimental apparatus is in progress.

E. Chemical Separations

1. Chemical-Metallurgical Process Studies

a. Chemistry of Liquid Metals

(i) Solubilities in Liquid Metal Solvents. The solubility of plutonium in liquid zinc has been determined over the temperature range from 458 to 752°C. Over this range, the solubility may be represented by the empirical equation

$$\log (\text{atom percent plutonium}) = 8.612 - 10090T^{-1} + 1.461 \times 10^6 \, T^{-2} \, .$$

The solubility of rhenium in liquid zinc at 750°C was determined in an exploratory experiment and was found to be <0.04 w/o. This may be compared with the solubilities of manganese and technetium, which were found to be 25 and 0.11 w/o, respectively, at 750°C. Thus, it is seen that for these elements the solubility decreases with increasing atomic number.

(ii) Plutonium-Cadmium Galvanic Cell Studies. The thermodynamics of the plutonium-cadmium system are being evaluated by means of galvanic cells. A cell of the form Pu|PuCl$_3$, LiCl-KCl (eutectic)|Pu-Cd (two-phase alloy) has been studied. The emf of the cell as a function of temperature can be represented by two empirical equations over the temperature range from 350 to 570°C:

$$(350 \text{ to } 403°C): \quad E \text{ (v)} = 0.69989 - 0.57459 \times 10^{-3} \text{ T}$$

with a standard deviation of 1 mv, and

$$(403 \text{ to } 570°C): \quad E \text{ (v)} = 0.57832 - 0.39488 \times 10^{-3} \text{ T}$$

with a standard deviation of 0.7 mv.

The temperature at the intersection of the two lines that represent these equations, 403°C, is in excellent agreement with the solubility data which indicate a peritectic at 404°C (see Progress Report for April 1963, ANL-6717, p. 52).

A plutonium-cadmium galvanic cell of the form

Pu| PuCl$_3$, KCl-LiCl (eutectic)|Pu-Cd (single phase)
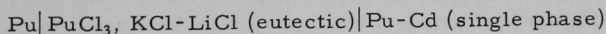
is also being used in the studies of the plutonium-cadmium system. This cell, in which the cathode is a single-phase alloy, permits the direct determination of the excess quantities $\overline{F}_{Pu}^{xs}$, $\overline{L}_{Pu}^{xs}$, and $\overline{S}_{Pu}^{xs}$ as a function of plutonium concentration. Analysis of preliminary data indicate that the values of both $\overline{L}_{Pu}^{xs}$ and $\overline{S}_{Pu}^{xs}$ are concentration dependent.

(iii) Study of Rare Earth-Cadmium System by the Effusion Balance Method. The studies of the phase relations in the rare earth-cadmium systems by the recording effusion balance method are being extended to include some representative heavy rare earth elements. Preliminary data have been obtained for the systems, dysprosium-cadmium and erbium-cadmium. In both systems the formation of the intermetallic phases MCd$_6$, M$_3$Cd$_{13}$, and MCd$_2$ was observed. It is probable that the MCd phase also occurs in these systems, although no direct observation was made because of the low effusion rates in this composition region.

b. Reduction of Thorium Dioxide. Scouting studies have been performed on crucible materials for thorium dioxide reduction. Reductions were carried out for 4 hr at 850°C, using magnesium fluoride magnesium chloride flux and magnesium-zinc alloy. Impurity levels in thorium metal prepared in four crucible materials were as follows:

Crucible Material	Impurity Level (%) in Product			
	W	C	Si	Al
Pressed-and-sintered Tungsten	N.D.*	0.025		
ATJ Graphite		0.34		
Silicon nitride-bonded silicon carbide		0.18	~1	
Norton Alundum 213		0.025		~1

*N.D. - Not detectable (<500 ppm)

Results showed that tungsten is a satisfactory crucible material from the standpoints of integrity and lack of product contamination, whereas use of any of the other three materials may result in contamination of the product.

2. Fluidization and Volatility Separations Processes

a. Fluoride Separations. The gamma decomposition of plutonium hexafluoride to plutonium tetrafluoride and fluorine in the presence of helium and krypton is being investigated. The results of current and previously reported experiments made with helium at 1 and 2 atm (see Progress Report for March 1963, ANL-6705, p. 50) have been used to calculate G values* for the decomposition of plutonium hexafluoride samples (at about 80 mm Hg pressure). The G values have been calculated on the basis of energy absorption in plutonium hexafluoride rather than on the basis of total energy absorption, which would also include the energy absorbed by the inert gas (see ANL-6705, p. 50). The G values obtained by the former method emphasize the striking similarity of the behavior of plutonium hexafluoride samples when irradiated in the presence of helium or alone. At absorbed energy doses (in plutonium hexafluoride alone) ranging from 8×10^{20} to 41×10^{20} ev, experiments with helium at 1 and 2 atm gave G values of 7.2 ± 1.1 and 5.8 ± 0.8, respectively. The amount of plutonium hexafluoride which decomposed appears to increase almost linearly with absorbed energy in the range studied. Combining the two values yields a G value of 6.6 ± 1. These G values may be compared with the value of 7.5 ± 0.7 obtained for plutonium hexafluoride when irradiated alone. These results indicate that helium exerts no significant influence on the decomposition of plutonium hexafluoride during gamma irradiation.

*Molecules decomposed per 100 ev of radiation.

In experiments made with krypton at pressures which were varied between 0.03 and 2 atm and with an absorbed energy (in plutonium hexafluoride alone) of about 15 x 10^{20} ev, the krypton produced a complex effect on the decomposition of plutonium hexafluoride. This effect appears to depend upon the electron fraction of krypton in the mixture of plutonium hexafluoride and krypton. In Figure 17, G values for the decomposition of plutonium hexafluoride samples (at about 80 mm Hg) are plotted against the electron fractions of krypton in the mixtures. It is seen that the G value falls from an initial value of 7.5 in the absence of krypton to a minimum of approximately 5.8 at an electron fraction of krypton of about 0.28. The G value then rises to a maximum value of greater than 15 at an electron fraction of krypton of app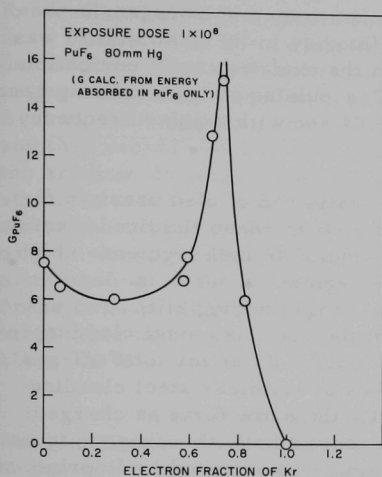roximately 0.75, and then falls sharply to zero. Further studies will be made in an effort to determine the mechanism whereby krypton affects the decomposition of plutonium hexafluoride.

Figure 17. Effect of Krypton on the Decomposition of PuF_6.

b.   Direct Fluorination of Uranium Dioxide Fuel. The development of a two-zone oxidation-fluorination scheme for the conversion of uranium dioxide pellets into uranium hexafluoride in a single reactor was continued in engineering-scale studies (see Progress Report for April 1963, ANL-6717, p. 55). In this scheme, there are two distinct reaction zones. The first is a bed of uranium dioxide pellets with alumina particles in the voids of the bed; the second is a bed of alumina particles placed over the uranium dioxide pellet bed. In the pellet bed zone, U_3O_8 fines are produced by contacting the uranium dioxide with an oxygen-nitrogen stream which also serves to fluidize the alumina particles. The U_3O_8 fines are elutriated from the lower zone and are reacted in the upper zone with fluorine, which is admitted to the fluidized bed of alumina just above the uranium dioxide pellet bed. The fluidized alumina not only serves as a heat transfer medium, but also appears to aid in the transport of the U_3O_8 fines to the fluorination zone.

Work has been started on the evaluation of the two-zone oxidation-fluorination scheme for the processing of stainless steel-clad pellets. To simulate sheared pieces of clad fuel elements, short lengths of stainless steel cladding with the ends left open were used to contain uranium dioxide pellets. Longer sections of fuel element, with longitudinal perforations or slits, were also evaluated.

Two runs were made to determine the completeness of removal of the uranium dioxide from the stainless steel cladding. The operating conditions for the two runs were as follows: in the oxidation zone, the composition of the fluidizing gases was 22 percent oxygen in nitrogen; in the fluorination zone, the concentration of the fluorine in the gas mixture was from 4 to 10 percent. The temperatures in the oxidation and fluorination zones were 450 and 500°C, respectively. Gas pulsing of the fluidizing gases was used in which the pulse duration was 0.04 sec with a pulse frequency of 2 pulses per minute.

In the first run, a 1.5-in.-deep static bed of clad uranium dioxide pellets (1.22 kg uranium dioxide) and a 20-in.-deep fluidized alumina zone (7.1 kg) were used. The charge consisted of 42 fuel segments which varied in length from about 1 to $1\frac{7}{8}$ in., one segment about 6 in. long (cladding slit), and one segment about 12 in. long (cladding slit). The uranium dioxide was completely removed from the stainless steel cladding in a total processing time of 8.5 hr, which included 3.25 hr for total off-gas recycle with fluorine. The 42 smaller pieces of stainless steel cladding were recovered from the reactor in virtually the same form as charged; in the case of the longer sections, however, only small, thin fragments were recovered. In all cases, the stainless cladding was attacked by fluorine, as was evident from surface scale formation. Bulging of the stainless steel tubing by the oxidation step was less severe than the bulging obtained in separate oxidation experiments.

In the second run, a 6-in.-deep static bed of clad pellets (3.48 kg uranium dioxide) and a 20-in.-deep fluidized alumina zone (7.1 kg) were used. The charge consisted of 175 one-in.-long fuel segments (two UO_2 pellets each). In this run, the uranium dioxide was 95 percent removed from the stainless steel cladding in a total processing time of 13.5 hr, which included 6.75 hr for total off-gas recycle with fluorine.

In the two runs, the removal of uranium dioxide from the stainless steel cladding was enhanced by the passage of recycled fluorine through the packed section.

c. Decladding of Fuel Elements by Fluid-bed Oxidation. Work is being continued on the development of a method for the removal of uranium dioxide pellets from stainless steel cladding by oxidation of uranium dioxide to a higher valence state in a fluidized bed. Studies thus far have been concerned with the direct oxidation of the uranium dioxide to uranosic oxide, U_3O_8. The conversion of the dioxide to U_3O_8 creates large internal stresses within the uranium dioxide pellets, because of the difference in densities of the two oxides, and results in the fragmentation of the pellets. The U_3O_8 fines that are formed in the reaction are elutriated from the pellet bed into the fluorination zone of the reactor by the oxidizing gas stream.

In previously reported engineering-scale runs (see Progress Report for April 1963, ANL-6717, p. 56), difficulty in obtaining complete physical removal of uranium dioxide from the cladding was encountered. Removals of up to 80 percent were achieved at rates that were considered to be reasonable. In an effort to achieve greater removals, the study of oxidation-reduction-reoxidation treatments has been undertaken. Four engineering-scale runs have been made in which the uranium dioxide was first oxidized with air, reduced with hydrogen (5 v/o hydrogen in nitrogen), and then reoxidized with air. This procedure favors the distinegration of the uranium dioxide pellets and has the probable advantage of leaving the stainless steel cladding intact, since the cladding does not react with either the oxygen or the hydrogen. In these runs, the fuel charge consisted of 1-in.-long by $\frac{1}{2}$-in.-diameter stainless steel cladding containing uranium dioxide. The ends of the cladding were open to simulate sheared fuel elements. In all runs, the initial oxidation and reoxidation temperatures were about 450°C, and the temperature of hydrogen reduction was about 550°C.

In two of the four runs, forty of the fuel segments were randomly packed in a 2-in.-diameter fluidized-bed reactor. The oxidation-reduction-reoxidation treatment in these two runs resulted in removals of only 80 percent of the uranium dioxide from the cladding. These removals are the same as those obtained previously by direct oxidation. The lack of improvement is attributed to insufficient circulation of the inert fluid-bed material and to insufficient motion of the individual fuel pieces. Gas pulsing (pulse duration of about 0.5 sec at a frequency of 2 pulses per minute), which was applied in one of the two runs, had no significant effect on the results.

In the other two runs, 32 fuel segments were charged to the 2-in.-diameter fluid-bed reactor. The fuel segments were used to make four individual beds, each about $1\frac{1}{2}$-in. deep, by separating the beds from each other by support plates. Gas pulsing (pulse duration, 0.5 sec; frequency, 2 pulses per minute) was used in both runs, and resulted in improved circulation of the inert bed material and greater motion of the fuel element pieces. Almost complete separations (99 and 100 percent) of the uranium oxides from the stainless steel cladding were achieved after a reaction time of about 13 hr. These results demonstrated that essentially complete separation of uranium dioxide from stainless steel cladding can be achieved by this treatment if the motion of the inert fluid bed material and especially the motion of the fuel pieces are not restricted.

d. Separation of Uranium from Zirconium and Aluminum Alloy Fuels.

(i) Fluid-bed Hydrolysis of Aluminum Tetrachloride. Engineering-scale studies were carried out to determine the feasibility of converting aluminum trichloride to aluminum oxide by hydrolysis with

steam as a means of handling the volatile aluminum trichloride in the off-gas during the hydrochlorination step of aluminum-based fuels. Three runs were carried out in a 6-in.-diameter reactor using an aluminum trichloride feed rate of 4 kg/hr and using a quantity of steam equivalent to four times the stoichiometric requirement.* Sand was used as the starting bed material. The temperature of the sand bed was 300°C. The three runs (total run time of 9.5 hr) were all completed satisfactorily and operation was troublefree. Good material balances (about 99 percent) were obtained. Aluminum was not found in the off-gas condensate stream, which indicated that hydrolysis of the aluminum trichloride to aluminum oxide was complete and that retention of the aluminum oxide solids by the sintered metal off-gas filters was very good.

(ii) <u>Pilot Plant for Processing Enriched Uranium-Zircaloy Alloy Fuels</u>. The installation of a pilot-plant facility to demonstrate the fluid-bed volatility process for reprocessing enriched uranium-zirconium alloy fuels has been completed. Final leak-testing of equipment is in progress. Operational testing of process equipment components (such as, the uranium hexafluoride cold-traps, the cooling system on the primary reactor, and the fuel-loading mechanism) remain to be done before initial shakedown runs are made. The experimental program will be carried out with nonirradiated fuel (up to 30 kg of alloy per charge). Separate tests using irradiated feed materials are being planned for a bench-scale facility which will be erected in a shielded cell.

3. <u>Calorimetry</u>

Development of analytical methods for the determination of the products of combustion of carbon and silicon carbide in fluorine has been essentially completed. A gas-chromatographic method has been developed for the analysis of the fluorocarbon products resulting from the combustion of carbon. Mass spectrometry will be used to determine whether complete conversion of silicon carbide to silicon tetrafluoride is obtained in the combustion of the carbide.

The value determined for the enthalpy of formation of crystalline uranium hexafluoride (see Progress Report for November 1962, ANL-6658, p. 56) has been recalculated. The revised value is $-522.5_7 \pm 0.4_4$ kcal/mole.

The determination of the standard thermal data for the formation of uranium hexafluoride makes it possible to measure enthalpies of formation of various uranium compounds for which adequate thermochemical data are not available. One of these compounds, uranium monosulfide, which is of interest in fast reactor technology, is being studied. Exploratory work has indicated that uranium monosulfide undergoes a slight reaction

---

*Based on the reaction $2AlCl_3 + 3H_2O \rightarrow Al_2O_3 + 6HCl$.

with fluorine at room temperature. It will be necessary, therefore, to protect the uranium monosulfide against exposure to fluorine prior to the intentional ignition of the sample. In preliminary combustions, essentially complete conversions of uranium monosulfide to volatile products (assumed to be uranium and sulfur hexafluoride) were obtained with samples weighing 0.8 to 1.4 gm when 10 to 15 atm of fluorine were used.

IV. ADVANCED SYSTEMS RESEARCH AND DEVELOPMENT

A. Argonne Advanced Research Reactor (AARR)

1. Facility Design

Preliminary studies have indicated the feasibility of obtaining maximum unperturbed thermal-neutron fluxes as high as 1×10^{16} n/(cm^2)(sec) by operating AARR at power levels up to 240 Mw (see Progress Report, for December 1962, ANL-6672). Consequently, the overall facility design has been modified and refined to incorporate greater flexibility for increasing the designed power level. These modifications have been carried out by the architectural firm of Shaw-Metz and Associates under a general Laboratory study subcontract.

The major change has been the elimination of the full sub-basement (equipment level) in the Reactor Building, and the addition of an Equipment Building to the adjacent Support and Services Complex. (The latter includes the Laboratory and Office Building, and the Equipment Storage and Mock-up Building.) Separate buildings for waste storage and treatment, and for air handling and filtration, have been eliminated.

Almost all of the equipment for the primary system, formerly located in the Reactor Building sub-basement, has been relocated to the lower level of the new Equipment Building. This lower level communicates directly with the Reactor Building canal floor level and forms a part of the containment volume of the reactor system, but is easily accessible for maintenance or for adding new equipment required for increasing the reactor power level. Other portions of the Equipment Building (not a part of the containment) provide space for all electrical switchgear, emergency standby units and batteries, Reactor Building air-conditioning units, air-handling and -filtration equipment, waste storage and treatment, and auxiliary systems. These changes result in a more compact arrangement that offers more efficient and flexible use of space, and requires less excavation and building volume below grade for the Reactor Building.

2. Core Physics

A calculational program to obtain the temperature dependence of the U^{235} cross section is complete except for final checking. This program is an extension of 1559/RE reported earlier. Temperature dependence in high-energy groups (above 100 ev) will be calculated by the narrow resonance approximation, while the low-lying resonances (1 to 100 ev) will be calculated more exactly by the techniques of 1559/RE.

3. Critical Experiment

A revised safety analysis report is being prepared. Procurement of fuel and other materials has been initiated.

4. Reactor Control Studies

a. <u>Transfer Functions for 50-30 Core</u>. Transfer-function representations of the AARR 50-30 (50 mil-thick fuel plates, spaced 30 mils apart) core have been calculated for various values of reactor power and, hence, for various inherent reactivity feedback functions. Digital codes RE/290 and SHARE ANCOOL were used to evaluate the pole-zero form of the transfer functions derivable from the conventional, point reactor, neutron kinetics, and appropriate thermal equations. Core-feedback functions and closed-loop transfer functions were calculated for nominal power levels of 0, 50, 100, and 150 Mw, through use of the material properties at those power levels. Values of the closed-loop function at power levels ranging from 12.5 to 250 Mw have also been calculated, the assumption being that there is only a linear variation in the amplitude of the feedback function with power.

In addition to their potential usefulness in determining the transient behavior and stability of the controlled reactor, the transfer functions provide further evidence of the inherent stability of the AARR core. Examination of the closed-loop expressions shows the poles to be confined to the negative real axis for the power levels considered. Linear extrapolation of the open-loop function determined for 150 Mw shows that no complex poles occur in the closed-loop function until power reaches approximately 400 Mw. However, this conclusion would be modified by the effects of increased feedback gain due to steam generation, which is neglected here.

b. <u>Analog Representation of Primary Coolant Loop</u>. Development of the equations necessary for characterization of the AARR primary coolant loop was continued. Pump equations wherein both the retarding impeller torque and developed pump head are assumed to be proportional to the square of the pump speed were used. These have yielded satisfactory results in coastdown and startup analyses, described by D. Burgreen, Nuclear Sci. and Eng., <u>6</u>, 306-312 (1959); <u>8</u> (1960), (Letter to the Editor).

Pipe runs for the primary loop were estimated, based on the latest plans (see Sect. IV.A.1 above) for location of the components contained therein. Pipe diameters were taken to be those as shown in the United Nuclear Corporation Preliminary Feasibility and Cost Study (UNC-5024). The loop thus formed was sectionalized into elements of constant diameter, for each of which water force balance and junction relationships were written. The location and dimensioning of the pressurizer system were considered as parameters in the loop equations, so that performance optimization studies may be made as these quantities are varied.

Analog programming of these primary loop equations, coupled with the existing core program, is proceeding.

5. Fuel and Core Designs

A reference mechanical design for the fuel and reactor-core structures has been selected. Gap tolerances between fuel assemblies and core structural members are to be held to less than 0.015 in. It is anticipated that achievement of such tolerances throughout the core will require bench assembly of the complete core, support plate, and shrouds, with subsequent loading of the complete unit core into the reactor vessel. Appropriate measures will, of course, be taken to maintain a wide margin of subcriticality of the core during all phases of assembly and transfer to the reactor vessel.

Techniques for fabrication of fuel assemblies of the reference design are being developed in the course of manufacture of two test assemblies (designated FTS-4 and -5), which will be used subsequently as samples in hydraulic experiments to determine the flow characteristics of the fuel assembly. Thus far, the fabrication methods selected appear well suited to the rhombic fuel-assembly configuration, and the necessary tolerances of ± 0.001 in. appear to be economically achievable.

6. Design of Experimental Facility Beam Tube

Preliminary stress calculations based on an isotropic flux distribution have been completed for the aluminum experimental facility beam tubes for AARR. These tubes penetrate the beryllium reflector surrounding the reactor core and terminate near the core at positions such as to achieve maximum thermal-neutron flux in the tubes for the use of experimenters. Thermal and pressure stresses for the cylinder and hemispherical end cap were computed for external pressures of 500 psig and 800 psig, and for tubes ranging in diameter from 2.75 in. to 6.25 in. The results indicate that the design is feasible with external cooling only for all pressures and tube diameters except the 6.25-in. tube.

Refined calculations accounting for geometry, differential circumferential heating, heat transfer, metal temperatures, and discontinuity stresses in the beam tubes have been outlined, and negotiations are currently in progress to subcontract this work with an outside firm well versed in this type of analysis. A complete study and analysis of the cooling requirements, profile temperatures, wall thickness, and stresses will be performed in order to establish the optimum design of the experimental beam tubes in the vicinity adjacent to the core.

B. Magnetohydrodynamics

1. MHD Power Generation

A study of the various heat transfer and fluid mechanical problem associated with a two-fluid (liquid metals) MHD cycle for nuclear-electric power conversion is being made. One of the essential features of such a cycle is the performance of the condenser unit. This unit should be designed so that it can operate in a zero-gravity environment as well as on earth without introducing additional moving parts. To this end, it is proposed that an electromagnetic field be used to increase terrestrial condensation rates and sustain (and initiate) zero-gravity condensation rates. A mathematical model has been postulated to describe such a system in a simple geometry in order to determine the efficiency of this technique. The equations are now being programmed for numerical solution.

Several other problems of MHD heat transfer are also being considered, but they are in early stages of analysis and/or computation. These problems include the effects of a magnetic field on the free convection of conducting fluids with nonuniform, unsteady thermal boundary conditions and the role of magnetohydrodynamics in combined free- and forced-convection heat transfer.

Equipment for calibrating water flow was assembled to provide a system for determining the operation of the thermocouple flowmeter described in ANL-6717 (Monthly Progress Report for April 1963, pp. 60). A series of calibration curves were obtained for temperatures up to 90°C. The results appeared to be reliable, and the instrument was installed in the plastic model of the injector-type MHD system and tested with water at 7 psig. Motion-picture photographs of this operation were taken, and these observations will be qualitatively correlated with the data obtained from the flowmeter.

V. NUCLEAR SAFETY

A. Thermal Reactor Safety Studies

1. Metal Oxidation and Ignition Studies

Ignition temperatures of foils and cubes of plutonium and plutonium alloys are being determined by the burning-curve method (see Progress Report for December 1962, ANL-6672, p. 41) and by shielded ignition experiments (see Chemical Engineering Division Summary Report for April, May, June, 1961, ANL-6379, p. 194). In the preceding Progress Report, the ignition temperatures of pure plutonium foils in air and in oxygen were tabulated as a function of the specific area of the sample (see ANL-6717, p. 63, Table VIII). The ignition temperatures were found to range from 520°C for a foil having a specific area of 5.3 sq cm/g to 280°C for a foil having a specific area of 6.7 sq cm/g or greater. However, a discontinuity was observed in the ignition temperatures at a specific area of about 5 sq cm/g for ignitions in oxygen and at about 1 sq cm/g for ignitions in air. From the ignition data for pure plutonium, it appears likely that two regimes are operative in the reactions leading to ignitions, one resulting in ignition temperatures of about 500°C and the other in temperatures of about 300°C. The occurrence of the two regimes has been tentatively attributed to the change in kinetics that was observed between 320 and 420°C in studies of the isothermal oxidation of plutonium (see Progress Report for March 1963, ANL-6705, p. 63).

The plutonium-ignition studies have been extended to include the determination of the ignition temperatures of binary alloys of plutonium. Thus far, alloys of plutonium with manganese, carbon, or aluminum, in which the concentration of the alloying element was about 2 atom percent, have been studied. The ignition temperatures of the alloys were determined as a function of the specific area of the samples, which were in the form of foils or cubes. The ignitions were carried out in air and in oxygen by both the burning-curve and shielded ignition methods. The results of these experiments are given in Table XVII.

The ignition data for the manganese-plutonium alloy are similar to those for pure plutonium except that the transition from the low-temperature regime to the high-temperature regime occurs at a specific area of 2 sq cm/g in both air and oxygen. Ignitions of the 0.10- and 0.07-mm-thick foils of the manganese-plutonium alloy were not observed in burning-curve experiments carried out in air. Because of the thinness of the foils in these two experiments, the metal was consumed before ignition could occur.

In the case of the carbon-plutonium alloys, the ignition temperatures obtained by the burning-curve method were slightly lower than the temperatures encountered in the high-temperature regime for pure plutonium.

Shielded experiments with oxygen produced ignition temperatures that were similar to those encountered in the low-temperature regime for plutonium. In no case did the carbon-plutonium alloy show a discontinuity in ignition temperatures.

Table XVII. Ignition Temperatures of Two a/o Plutonium Alloys

Alloy	Foil Thickness (mm)	Specific Area (sq cm/g)	Burning-curve Ignition Temperature (°C)		Shielded Ignition Temperature (°C)[a]	
			Air	O₂	Air	O₂
Manganese	5 (cube)	0.66	499	477		
	1.0	1.6	496	483	362-406	249-294
	0.53	2.7	293	320	221-258	240-288
	0.24	5.3	365[b] 598[b]	293	257-288	276-300
	0.21	5.6	330	247		214-230
	0.10	12.1	No ignition[c]	289	282-317	242-278
	0.07	17.2	No ignition[c]	279	251-258	251-282
Carbon	5 (cube)	0.65	498	486		
	0.97	1.6	474	478	401-440	287-328
	0.28	4.1				270-300
	0.16	7.8	469	466	386-428	275-309
Aluminum	5 (cube)	0.79	588, 590	576		
	0.26	4.4	554	555		350-388
	0.26	4.8	557	546	350-388	375-407

[a]Indicated as the highest temperature at which ignition did not occur and the lowest temperature at which ignition did occur.

[b]This particular foil indicated a burning-curve ignition temperature in air on the recorder and visually at 598°C. A repeat of the same experiment gave an observed ignition in the 365°C region. However, no appreciable temperature rise was recorded, possibly due to poor contact of sample to thermocouple.

[c]Sample completely oxidized or disintegrated before ignition occurred.

The aluminum-plutonium alloy was found to ignite about 60 to 100°C above the high-temperature regime for plutonium. From the data obtained with the two types of samples (a 5-mm cube and a 0.26-mm-thick foil) employed in this study, no judgment can be made concerning the existence of a discontinuity in the ignition temperatures of aluminum-plutonium alloys.

2. Metal-Water Studies

a. Application of Laser-beam Heating to Metal-Water Reactions. Preparations are being made to apply heating by a laser beam to metal-water studies. It is hoped that this method will permit the heating of a

single small particle of metal to temperatures up to 3000°C while the particle is submerged in water. Spherical samples (about 1 mm in diameter) of uranium, zirconium, stainless steel, and aluminum have been prepared by melting wire stock. Uranium and stainless steel discs ($\frac{1}{32}$ and $\frac{1}{16}$ in. in diameter) have been prepared as punchings from foil.

b. <u>Reaction of Stainless Steel with Steam.</u> Studies of the isothermal reaction of Type 304 stainless steel with steam have been started. The results of experiments carried out at 1100 and 1300°C indicate that the oxidation reaction followed a parabolic rate law at 1100°C and a paralinear rate law at 1300°C. In an experiment at 1500°C, the integrity of the oxide shell, which is formed first and which serves as a container for the molten metal, was lost. The resulting collapse of the specimen negated the experiment.

c. <u>Metal-Water Reactions in TREAT.</u> Four in-pile experiments in TREAT were completed. In two experiments, aluminum-clad SPERT 1-D-type aluminum-uranium alloy fuel specimens were used. In the other two experiments, unclad SL-1-type aluminum-uranium fuel specimens were employed. The specimens, which were submerged in water, were contained in specially constructed autoclaves and were heated to 285°C prior to exposure to a neutron pulse. The SPERT 1-D plates were subjected to nuclear energy inputs of 390 and 570 cal/g. The SL-1 specimens received energy inputs of 350 and 500 cal/g. At the inputs of lower energy, the extent of reaction was 0.35 and 0.24 percent for SPERT 1-D and SL-1 samples, respectively. At the higher-energy inputs, 89 percent of the SPERT 1-D sample and 76 percent of the SL-1 sample reacted. The extent of the reactions at the higher-energy inputs was considerably greater than in corresponding runs carried out previously in room-temperature water. In the latter runs, the extent of reaction for equivalent energy inputs was less than 20 percent. Although the causes underlying these large differences in reaction rates are not yet known, it is thought that they may be related, not only to differences in pressures in the autoclaves, but also to the much greater heat losses involved in subcooled boiling (room-temperature water) than in saturated boiling (heated water). This difference in heat loss may have the effect of greatly diminishing the net energy input to specimens in room-temperature water.

B. <u>Fast Reactor Safety Studies</u>

1. <u>Experiments</u>

RE Series 36 was completed, and the samples were returned to Argonne, Illinois, for examination. This series consisted of four experiments using Fermi I-type fuel pins that had previously been irradiated to a burnup of approximately 0.5%.

Uranium sulfide samples 6 and 7 of RE Series 34 were irradiated and returned to Argonne, Illinois, for examination.

The series of experiments studying the penetration rate of Type 304 stainless steel by uranium and uranium-5% fissium alloy was continued with the irradiation of one sample in a transparent capsule.

Four dry capsules were remotely loaded with APDA irradiated fuel elements and subjected to excursions in the TREAT reactor. The conditions of the test and description of the decanned fuel elements are described in Table XVIII. The fuel composition consisted of an alloy of 90% uranium-10% molybdenum in which the uranium was enriched to 10% U^{235}. The elements were clad with 4 mils of zirconium by the co-entrusion process and were irradiated to about 0.5% burnup.

Table XVIII. Description of Irradiated APDA Fuel Elements Exposed to TREAT Transients

Capsule No.	Excursion (Mw-sec)	Approximate Clad Temp (°C)	Appearance of Fuel
9	29	1125	Split diameter increased from 0.157 in. to 0.193 in. at split.
10	26	1100	Warped diameter 0.159 in. throughout its length.
11	32.7	1185	Split lower two-thirds of length. Fuel partially ran out and solidified.
12	22.1	990	Warped diameter 0.157 in. to 0.1584 in.

2. TREAT Meltdown-experiment Analysis

Calculations are being made of energy releases during a major accident to a fast reactor caused by molten uranium metal squirting out of the center of the fuel pins, a phenomena observed in the TREAT experiments.

Preliminary calculations indicate that this type of accident can occur in three phases: (1) autocatalytic insertion of reactivity; (2) reactivity insertion at a constant rate; and (3) reactivity reduction by the Bethe-Tait-type mechanism.

The first phase lasts until the period reaches a value equivalent to the core radius divided by the velocity of sound in uranium. The excess reactivity is then about 10¢ above prompt critical. During the second stage, the reactivity will increase by factors of one to three. The amount of heat generated depends strongly on the amount of voids present at the beginning of the third stage.

Conditions at the beginning of the accident do not seem important in the terms of overall energy yield. However, the (rather difficult to pin down) mechanical condition of the core at the end of the first stage and the uncertainty in constants governing motion of the metal can easily affect the energy yield by a factor of two to three.

C. TREAT

1. Large TREAT Loop

During the past month, several revisions were made in the design of the large TREAT loop. The changes were made in the design of the "hydropad" transient excursion container, shielding blocks, mounting of the pressure transducer in the lower assembly, Conoseal flange, lifting head, and cask length.

In addition to the above design changes, a number of purchases are being processed and include:

(1) modifications to the 4-in. De Var ball valves; and

(2) bid evaluation for a number of stainless steel vessels.

(3) Bid packages are being prepared to cover the procurement of the safety heads required for the gas system and the cold trap assembly.

Further, a contract with the Franklin Institute to perform thermal-stress analysis in the loop has been approved. The work is scheduled to start late this month.

2. Effect of Sodium Oxide in Sodium Loops

A stainless steel loop designed to operate at ~800°C is practically complete. A glove box, designed to permit samples to be inserted in the loop, is being constructed by a vendor.

The sodium-conditioning loop to be used for testing the Blake meter is about two-thirds complete. (The Blake meter is an instrument for continually analyzing sodium oxide in a circulating sodium system.)

VI. PUBLICATIONS

Papers

NEUTRON RADIOGRAPHIC INSPECTION OF RADIOACTIVE IRRADI-
ATED REACTOR FUEL SPECIMENS
Harold Berger and W. N. Beck
Nuclear Sci. and Eng. 15 411-414 (April 1963)

PREPARATION AND PROPERTIES OF URANIUM AND THORIUM
MONOSULFIDES
P. D. Shalek
J. Am. Ceram Soc. 46 155-161 (April 1963)

PHASE STUDIES IN THE BINARY SYSTEM $MgO-Ta_2O_5$
Y. Baskin and D. C. Schell
J. Am. Ceram Soc. 46 (4) 174-177 (April 1963)

RESOLUTION STUDY OF PHOTOGRAPHIC THERMAL NEUTRON
IMAGE DETECTORS
Harold Berger
J. Appl. Phys. 34 914-918 (April 1963)

PERFORMANCE OF ALUMINUM-URANIUM ALLOY FUEL PLATES
UNDER HIGH TEMPERATURE AND HIGH BURNUP CONDITIONS
J. H. Kittel, A. P. Gavin, C. C. Crothers and R. Carlander
Research Reactor Fuel Element Conference, September 17-19,
1962, Gatlinburg, Tennessee, TID-7642, Book 2, pp. 425-433
(1963)

APPLICATIONS OF SCINTILLATION SPECTROMETRY TO RESEARCH
REACTOR FUEL ASSAY
Ronald B. Perry
Research Reactor Fuel Element Conference, September 17-19,
1962, Gatlinburg, Tennessee, TID-7642, Book 2, pp. 716-733
(1963)

AN EVALUATION OF FAST, SCINTILLATOR-POLAROID FILM
CAMERA FOR NEUTRON IMAGE DETECTION
Harold Berger and I. R. Kraska
Nondestruc. Testing XXI (3) pp. 181-184 (May-June 1963)

IRRADIATION OF METAL-FIBER REINFORCED THORIA-URANIA
L. A. Neimark, J. H. Kittel and C. L. Hoenig
J. Am. Ceram. Soc. 46, 219-224 (May 1963)

INFLUENCE OF OXYGEN ON HIGH TEMPERATURE AQUEOUS COR-
ROSION OF IRON
W. E. Ruther and R. K. Hart
Corrosion 19 (4), 127t-133t (April 1963)

FLUORINE BOMB CALORIMETRY: V. THE HEAT OF FORMATION
OF SILICON TETRAFLUORIDE AND SILICA
J. L. Margrave, H. M. Feder and W. N. Hubbard
J. Phys. Chem. 67, 815 (1963)

THE DECOMPOSITION OF PLUTONIUM HEXAFLUORIDE BY
RADIATION   Abstract
M. J. Steindler, R. P. Wagner and J. Fischer
Abstracts of Papers Presented at Am. Chem. Soc. Meeting,
Los Angeles, March 31 - April 5, p. 41P (1963)

INTERMEDIATE PHASES IN THE SYSTEMS La-Zn, Ce-Zn, Pr-Zn,
AND Nd-Zn   Abstract
E. Veleckis, I. Johnson and H. M. Feder
Abstracts of Papers Presented at Am. Chem. Soc. Meeting,
Los Angeles, March 31 - April 5, p. 15K (1963)

DELTA MODULATION AS A POSSIBLE SERVO DATA LINK
R. H. Maschhoff
Proceedings of the 1963 National Telemetering Conference,
May 20-22, 1963, Section 10-5 (1963)

AN AUTOMATIC RAPID SCANNING SPECTROPHOTOMETER TO
STUDY THERMOLUMINESCENCE SPECTRA
A. K. Ghosh
Applied Optics, 2, 3, 243-244 (March 1963)

Transactions of the American Nuclear Society, Vol. 6, No. 1 (June, 1963)
1963 Annual Meeting, Salt Lake City, Utah. June 17-19, 1963   Abstracts

ENHANCEMENT OF EXPERIMENTERS' FLUXES IN THE ARGONNE
ADVANCED RESEARCH REACTOR (AARR)
C. N. Kelber
pp. 5-6

ACTIVATION FOIL MEASUREMENTS OF NEUTRON FLUX DISTRI-
BUTION IN EBWR DURING POWER OPERATION
William G. Knapp
pp. 33-34

COMPUTATION OF RESONANCE LINE SHAPE FUNCTIONS
D. M. O'Shea and Henry C. Thacher, Jr.
pp. 36-37

Book Review

1960 NUCLEAR DATA TABLES; PART 4, SHORT TABLES. Compiled by K. Way, et al., Superintendent of Documents, U. S. Government Printing Office.
　　A. B. Smith
　　　　Nuclear Sci. and Eng. 16, 143-145 (May, 1963).

Books

NUCLEAR REACTOR CONTROL ENGINEERING
　　J. M. Harrer
　　　　D. Van Nostrand Company, Inc., Princeton, N. J., 1963.

ANL Reports

ANL-6675　　NUCLEATE BOILING CHARACTERISTICS AND THE CRITICAL HEAT FLUX OCCURRENCE IN SUBCOOLED AXIAL-FLOW WATER SYSTEMS
　　　　　　R. J. Weatherhead

　　　　　　NEUTRON RESONANCE INTEGRAL AND AGE DATA, Reactor Physics Constants Center Newsletter No. 10
　　　　　　P. J. Persiani, J. J. Kaganove, and A. E. McArthy